Furthermore, the cell death of Neuro2a cells induced by oxidative stress with 0.4 mM H_2O_2 was dramatically rescued by over-expression of wild-type DJ-1, but not by that of L166P mutant DJ-1 (Figs. 2A and B). The expressions of wild type and mutant DJ-1 proteins were confirmed by GFP-fluorescence (data not shown). In contrast, over-expression of DJ-1 did not influence the cell death caused by 0.2 mM staurosporin (Fig. 2C).

ER stress was given to the cells with tunicamycin and thapsigargin. ER stress-induced cell deaths of Neuro2a cells were also enhanced by down regulation of endogenous DJ-1 expression by the siRNA (Fig. 3A). At higher concentration of tunicamycin (5.0 μg/ml) and thapsigargin (5.0 μM), the induced cell death was decreased by over-expression of wild-type DJ-1, but not by that of L166P mutant DJ-1 (Fig. 3B, left). This rescue effect of DJ-1 overexpression on ER stress-induced cell death, however, is much less than that on oxidative stress-induced cell death. Unexpectedly, at lower concentration of tunicamycin (1.0 μg/ml) and thapsigargin (2.5 μM), over-expression of L166P DJ-1 seems to have a toxic effect (Fig. 3B, right).

Proteasome inhibition was made with lactacystin. The cell death induced by lactacystin was enhanced after down regulation of endogenous DJ-1 of Neuro2a cells by siRNA (Fig. 4A). At higher concentration of lactacystin (50 μM) the induced cell death was decreased by over-expression of wild-type DJ-1, but not by that of L166P mutant DJ-1. In contrast, at higher concentration of lactacystin (20 μM) the over-expression of L166P DJ-1 seems to be mildly toxic to the cells (Fig. 4B).

Putative G protein-coupled transmembrane polypeptide receptor (Pael R) was identified as an interacting protein of Parkin, another gene product of AR-JP [16]. Cell death of Neuro2a cells induced by over-expression of Pael R was rescued by co-expressed DJ-1 (Fig. 5).

All above results were confirmed by three independent experiments. The similar results were also obtained with 293T cells except for experiments with lower concentration of tunicamycin, thapsigargin, and lactacystin (data not shown).

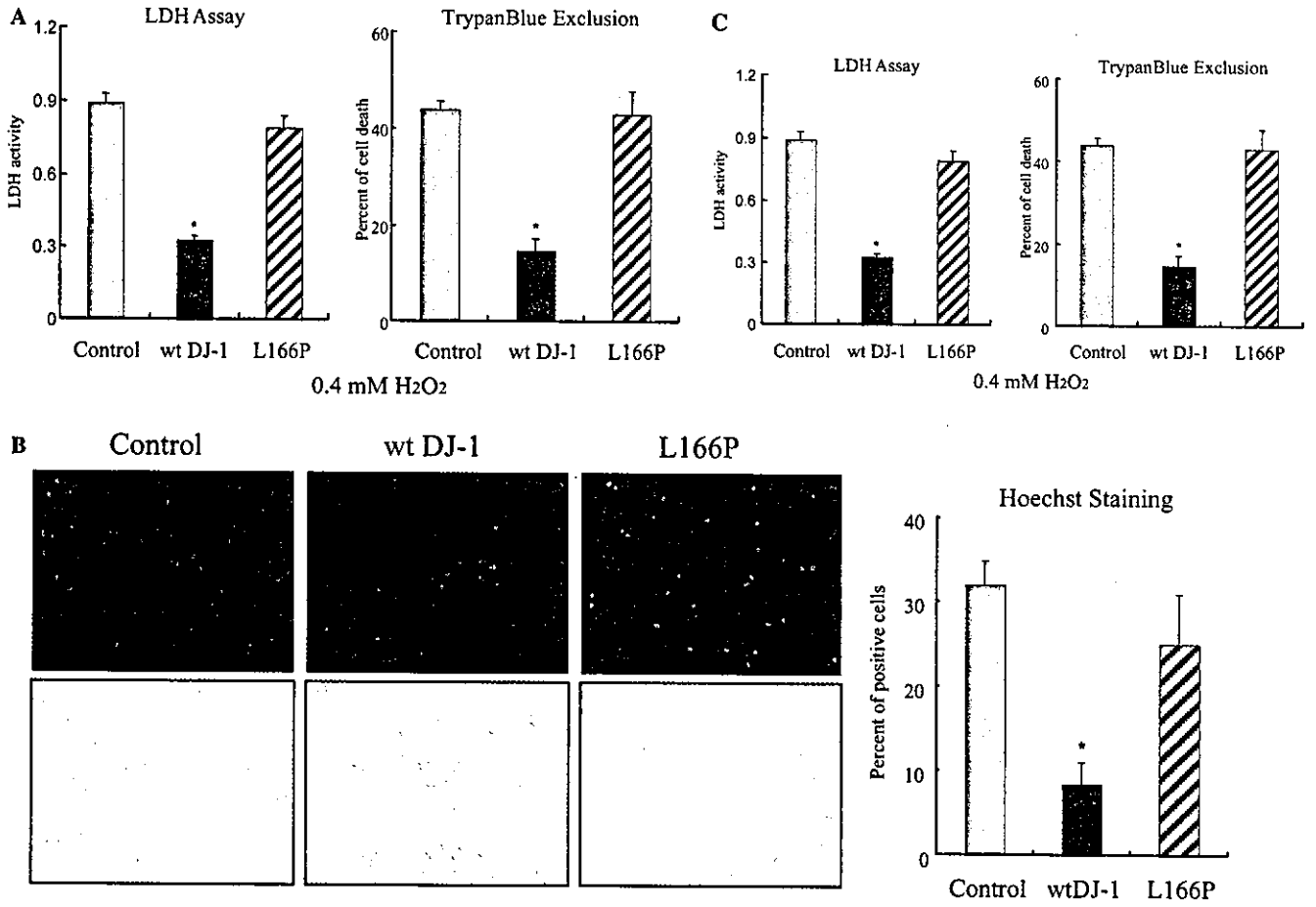

Fig. 2. Effect of DJ-1 over-expression on cell death induced by oxidative stress with H_2O_2. (A) The cell death of Neuro2a induced by 0.4 mM H_2O_2 was rescued by over-expression of wild-type DJ-1, not by that of L166P mutant DJ-1. $p < 0.001$. (B) Nuclear condensation of Neuro2a cells by Hoechst dye staining was much reduced by over-expression of wild-type DJ-1, not by that of L166P mutant DJ-1. The lower panels were pictures under light field. $p < 0.001$. (C) Over-expression of wild-type DJ-1 did not influence the apoptosis of Neuro2a induced by 0.2 mM staurosporin. NS, not significant.

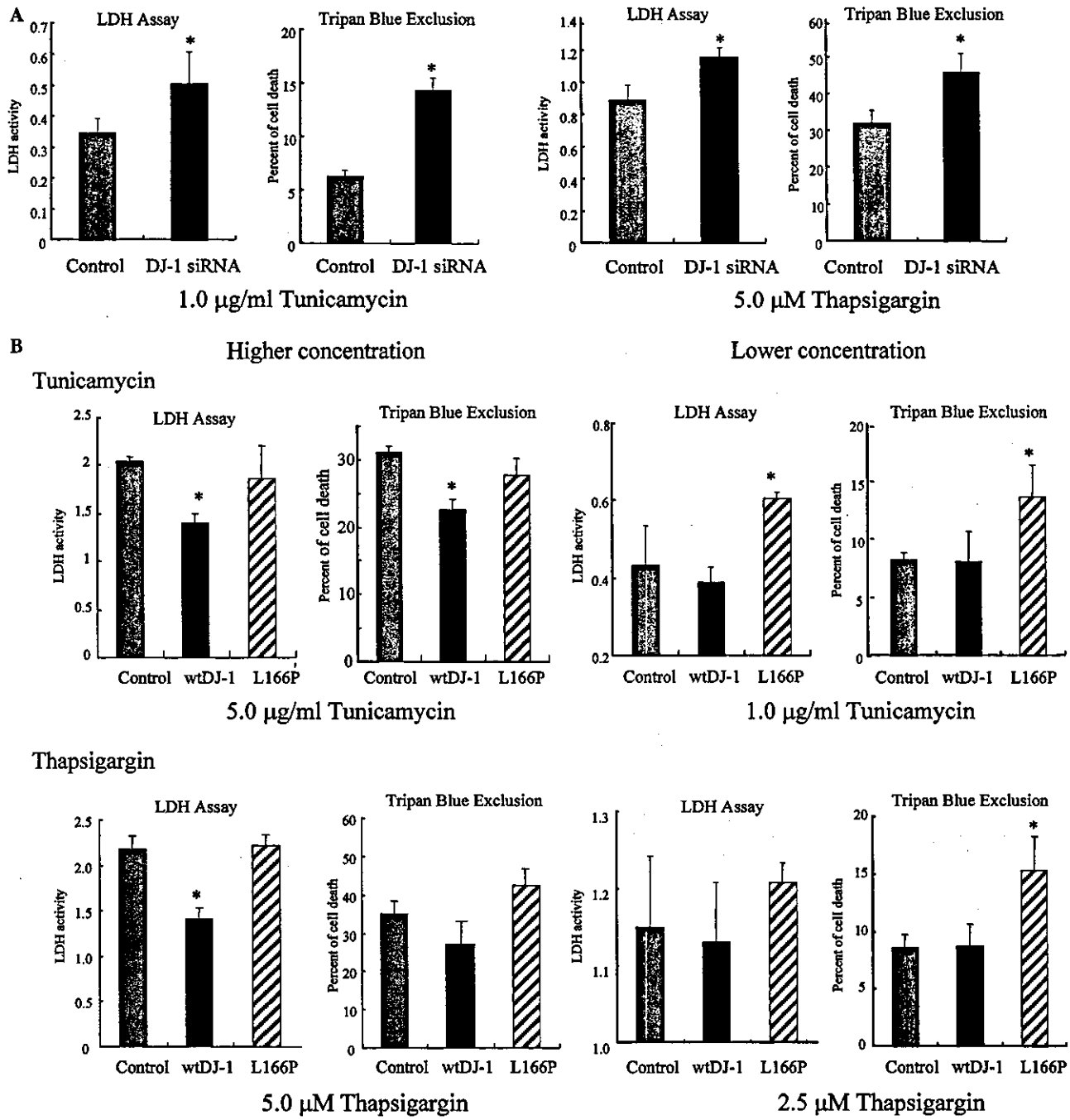

Fig. 3. Effect of DJ-1 down regulation or over-expression on cell death induced by ER stress. (A) Effect of down regulation of endogenous DJ-1 on cell death induced by ER stress. Knockdown of endogenous DJ-1 by siRNA increased cell death of Neuro2a induced by 1.0 μg/ml tunicamycin ($p < 0.01$) and that by 5.0 μM thapsigargin ($p < 0.05$). (B) Effect of DJ-1 over-expression on cell death induced by ER stress. Left panels: at higher concentration of tunicamycin (5.0 μg/ml, $p < 0.01$) and thapsigargin (5.0 μM, $p < 0.05$ only for LDH assay) cell death was decreased by over-expression of wild-type DJ-1, not by that of L166P DJ-1. Right panels: at lower concentration of tunicamycin (1.0 μg/ml, $p < 0.01$) and thapsigargin (2.5 μM, $p < 0.05$ only for trypan blue exclusion), over-expression of L166P DJ-1 tends to have toxic effect.

Discussion

Homozygous deletion, missense mutations (L166P, M26I), and compound heterozygous mutation in DJ-1 gene have been reported to be directly pathogenic for the phenotype of AR-EOP [2,8,9]. A homozygous 14 kb large deletion removing exons 1–5 [2], and a compound heterozygous mutation leading to the frameshift in the exon 1 and the splice error in exon 7 [8], both are predicted to result in a loss of functional protein. Recently, L166P DJ-1 protein proved to be unstable and rapidly degraded when expressed in

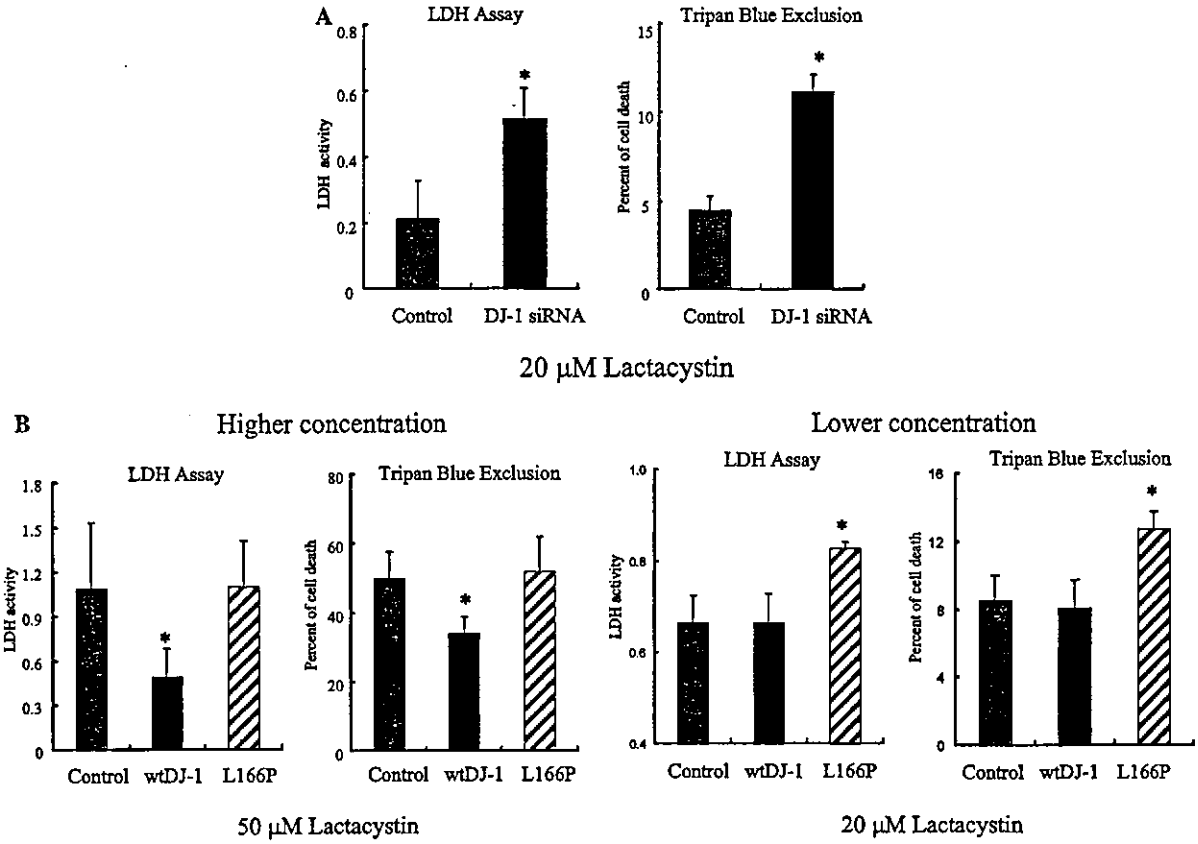

Fig. 4. Effect of DJ-1 down regulation or over-expression on cell death induced by proteasome inhibition with lactacystin. (A) Knockdown of endogenous DJ-1 by siRNA increased cell death of Neuro2a induced with 20 μM lactacystin ($p < 0.01$). (B) Effect of DJ-1 over-expression on cell death induced by lactacystin. Left: at higher concentration of lactacystin (50 μM), cell death was decreased by over-expression of wild-type DJ-1 ($p < 0.01$), not by that of L166P DJ-1. Right: at lower concentration of lactacystin (20 μM), over-expression of L166P DJ-1 tends to have a toxic effect. $p < 0.05$.

culture cells, and the level of L166P DJ-1 protein in patient's lymphoblasts, actually, was very low as compared to the wild type protein [10,11]. Therefore, in at least AR-EOP with mutant DJ-1, loss or reduction of DJ-1 protein function has been considered to cause the phenotype.

The pathophysiology of PD has not been well known, but oxidative stress is suggested to participate in the process of dopaminergic neuronal cell death that undergoes selective degeneration in PD (see recent review, [12]). Ferrous iron (Fe^{2+}) level is elevated and glutathione level is decreased in the substantia nigra, the dopamine-containing region of the brain, in patients with the disorder [13,14]. Accessible iron can react with H_2O_2 produced during oxidative deamination of dopamine to generate hydroxyl radicals ($^{\cdot}OH$) that can damage proteins, nucleic acids, and membrane phospholipids, leading to cellular degeneration [15]. We showed that neuronal cell death induced by H_2O_2 was enhanced by down regulation of endogenous DJ-1 and was dramatically rescued by over-expression of wild-type DJ-1 but not by that of L166P mutant DJ-1. These results suggest that DJ-1 works as a powerful antioxidant and that loss of its activity is related to dopaminergic neuronal cell death in patients with DJ-1 mutation.

There are several pieces of evidences suggesting that cell death in PD is related to ER-stress and proteasome inhibition. ER-stress maker protein, BiP, was up-regulated in AR-JP (PARK2) brain tissue compared with controls [16]. Parkin protein is E2-dependent E3 ubiquitin–protein ligase and its mutant lost the E3 activity [17]. Over-expression of mutant alpha-synuclein, causative mutation for autosomal dominant PD, produced a proteasome inhibition and sensitized the culture cells to toxicity induced by lactacystin [18,19]. Antisense knockdown of Parkin, another causative gene for autosomal recessive Parkinsonism, increased sensitivity to proteasome inhibitors [20]. Over-expression of Parkin, but not its mutant, specifically suppressed ER-stress-induced cell death [17].

Similar to the results with Parkin, in this study, the cell deaths of Neuro2a induced by ER-stress and proteasome inhibition were enhanced by down regulation of endogenous DJ-1 and slightly suppressed by DJ-1 over-expression. These results suggest that loss of DJ-1 protein activity makes neurons to be vulnerable to ER-stress or

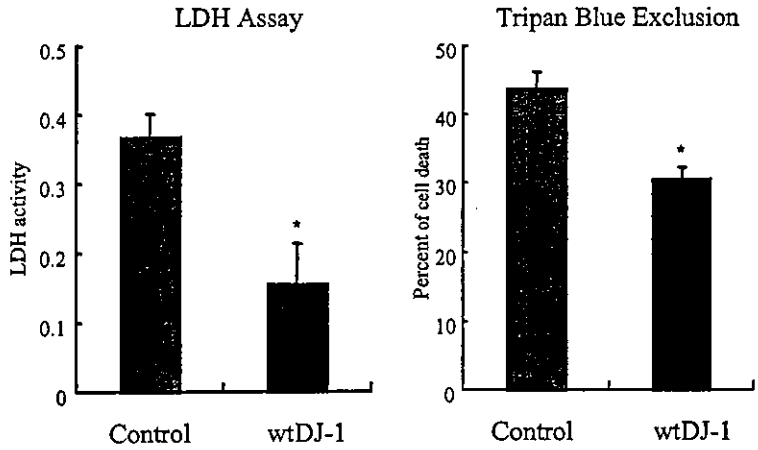

Fig. 5. Effect of DJ-1 over-expression on cell death induced by Pael R over-expression. Cell death was analyzed after co-transfection of 0.3 μg of Pael-R-expressing vector and 0.6 μg wild-type DJ-1 expressing vector (Neuro2a cells in 24 well). Over-expression of DJ-1 rescued cell death induced by Pael R expression ($p < 0.01$). In mock transfection with 0.3 μg pcDNA3.1 (Invitrogen) and 0.6 μg pEGFP-N1, the background cell death showed less than 0.06 in LDH activity and less than 4% in trypan blue exclusion method (data not shown).

proteasome inhibition. The protective activity of DJ-1 from ER stress might be attributed, at least in part, to anti-oxidant activity of DJ-1, because ER stress leads to accumulate endogenous peroxides and promotes oxidative stress [21]. Unexpectedly, at lower concentration of tunicamycin, thapsigargin, and lactacystin, over-expression of L166P mutant DJ-1 not only lost protective activity to these stresses, but also seemed to have a toxic effect on the cells. This mechanism is not known, but an aberrant DJ-1 protein might act in a dominant manner, because heterozygous missense mutations were found in sporadic Parkinson's disease [8,9]. However, further studies are needed to make clear the pathological mechanism of missense mutant DJ-1 under ER-stress and proteasome inhibition.

Pael R is a substrate of Parkin, E3 ubiquitin–protein ligase. Over-expression of parkin, but not mutant, reduced accumulation of insoluble Pael R and suppressed Pael-R-induced cell death. Furthermore, Pael R in insoluble fraction was actually increased in AR-JP brains compared with normal controls. The accumulation of unfolded Pael R is therefore suspected to be causative in AR-JP [16]. Here, DJ-1 over-expression rescues Pael-R-induced cell death. This result also supports that DJ-1 is related to neuronal cell death in patients with Parkinsonism.

In conclusion, our results suggest DJ-1 functions in protecting neuron from oxidative stress and ER stress, and that loss of these activities in mutant DJ-1 contributes to the pathophysiology in AR-EOP.

Acknowledgment

This work was supported by grants from the Ministry of Education, Science and Culture of Japan, and from Ministry of Health, Labour and Welfare of Japan.

References

[1] T. Kitada, S. Asakaw, N. Hattori, H. Matsumin, Y. Yamamura, S. Minoshima, M. Yokochi, Y. Mizuno, N. Shimizu, Mutations in the parkin gene cause autosomal recessive juvenile parkinsonism, Nature 392 (1998) 605–608.

[2] V. Bonifati, P. Rizzu, M.J. van Baren, O. Schaap, G.J. Breedveld, E. Krieger, M.C. Dekker, F. Squitieri, P. Ibanez, M. Joosse, J.W. van Dongen, N. Vanacore, J.C. van Swieten, A. Brice, G. Meco, C.M. van Duijn, B.A. Oostra, P. Heutink, Mutations in the DJ-1 gene associated with autosomal recessive early-onset parkinsonism, Science 299 (2003) 256–259.

[3] D. Nagakubo, T. Taira, H. Kitaura, M. Ikeda, K. Tamai, S.M. Iguchi-Ariga, H. Ariga, DJ-1, a novel oncogene which transforms mouse NIH3T3 cells in cooperation with ras, Biochem. Biophys. Res. Commun. 231 (1997) 509–513.

[4] A. Mitsumoto, Y. Nakagawa, DJ-1 is an indicator for endogenous reactive oxygen species elicited by endotoxin, Free Radic. Res. 35 (2001) 885–893.

[5] K. Takahashi, T. Taira, T. Niki, C. Seino, S.M.M. Iguchi-Ariga, H. Ariga, DJ-1 positively regulates the androgen receptor by impairing the binding of PIASxa to the receptor, J. Biol. Chem. 276 (2001) 37556–37563.

[6] T. Yokota, N. Sakamoto, N. Enomto, Y. Tanabe, M. Miyagishi, S. Maekawa, Y. Li, M. Kurosaki, K. Taira, M. Watanabe, H. Mizusawa, Inhibition of intracellular hepatitis C virus replication by synthetic and vector-derived small interfering RNAs, EMBO Rep. (2003) 602–608.

[7] M. Okada, K. Matsumoto, T. Niki, T. Taira, S.M.M. Iguchi-Ariga, H. Ariga, DJ-1, a target protein for an endocrine disrupter, participates in the fertilization in mice, Biol. Pharm. Bull. 25 (2002) 853–856.

[8] S. Hague, E. Rogaeva, D. Hernande, C. Gulick, A. Singleton, M. Hanson, J. Johnson, R. Weiser, M. Gallardo, B. Ravina, K. Gwinn-Hardy, A. Crawley, P.H. St George-Hyslop, A.E. Lang, P. Heutink, V. Bonifati, J. Hardy, A. Singleton, Early-onset Parkinson's disease caused by a compound heterozygous DJ-1 mutation, Ann. Neurol. 54 (2003) 271–274.

[9] P.M. Abou-Sleiman, D.G. Healy, N. Quinn, A.J. Lees, N.W. Wood, The role of pathogenic DJ-1 mutations in Parkinson's disease, Ann. Neurol. 54 (2003) 283–286.

[10] D.W. Miller, R. Ahmad, S. Hague, M.J. Baptist, R. Canet-Avile, C. McLendon, C.M. Carte, P.P. Zhu, J. Stadler, J. Chandran, G.R. Klinefelter, C. Blackstone, M.R. Cookson, Related L166P

mutant DJ-1, causative for recessive Parkinson's disease, is degraded through the ubiquitin–proteasome system, J. Biol. Chem. 278 (2003) 36588–36595.
[11] M.G. Macedo, B. Anar, I.F. Bronner, M. Cannella, F. Squitieri, V. Bonifati, A. Hoogeveen, P. Heutink, P. Rizzu, The DJ-1L166P mutant protein associated with early onset Parkinson's disease is unstable and forms higher protein complexes, Hum. Mol. Genet. 12 (2003) 2807–2816.
[12] P. Jenner, Oxidative stress in Parkinson's disease, Ann. Neurol. 53 (Suppl. 3) (2003) S26–S36.
[13] P.D. Griffiths, B.R. Dobson, G.R. Jones, D.T. Clarke, Iron in the basal ganglia in Parkinson's disease. An in vitro study using extended X-ray absorption fine structure and cryo-electron microscopy, Brain 122 (1999) 667–673.
[14] J.K. Andersen, Do alterations in glutathione and iron levels contribute to pathology associated with Parkinson's disease?, in: Ageing Vulnerability: Causes and Interventions, Novartis Foundation Symposium, vol. 235, Wiley, New York, 2001, pp. 11–25.
[15] J.M.C. Gutteridge, Iron and oxygen radicals in brain, Ann. Neurol. 32 (1992) S16–S21.
[16] Y. Imai, M. Soda, H. Inoue, N. Hattori, Y. Mizuno, R. Takahashi, An unfolded putative transmembrane polypeptide, which can lead to endoplasmic reticulum stress, is a substrate of Parkin, Cell 105 (2001) 891–902.
[17] Y. Imai, M. Soda, R. Takahashi, Parkin suppresses unfolded protein stress-induced cell death through its E3 ubiquitin-protein ligase activity, J. Biol. Chem. 275 (2000) 35661–35664.
[18] L. Stefanis, K.E. Larsen, H.J. Rideout, D. Sulzer, L.A. Greene, Expression of A53T mutant but not wild-type alpha-synuclein in PC12 cells induces alterations of the ubiquitin-dependent degradation system, loss of dopamine release, and autophagic cell death, J. Neurosci. 21 (2001) 9549–9560.
[19] Y. Tanaka, S. Engelender, S. Igarashi, R.K. Rao, T. Wanner, R.E. Tanzi, A.L. Sawa, V. Dawson, T.M. Dawson, C.A. Ross, Inducible expression of mutant alpha-synuclein decreases proteasome activity and increases sensitivity to mitochondria-dependent apoptosis, Hum. Mol. Genet. 10 (2001) 919–926.
[20] L. Petrucelli, C. O'Farrell, P.J. Lockhart, M. Baptist, K. Kehoe, L. Vink, P. Choi, B. Wolozin, M. Farrer, J. Hardy, M.R. Cookson, Parkin protects against the toxicity associated with mutant alpha-synuclein: proteasome dysfunction selectively affects catecholaminergic neurons, Neuron 36 (2002) 1007–1019.
[21] H.P. Harding, Y. Zhang, H. Zeng, I. Novoa, P.D. Lu, M. Calfon, N. Sadri, C. Yun, B. Popko, R. Paules, D.F. Stojdl, J.C. Bell, T. Hettmann, J.M. Leiden, D. Ron, An integrated stress response regulates amino acid metabolism and resistance to oxidative stress, Mol. Cell. 11 (2003) 619–633.

Available online at www.sciencedirect.com
SCIENCE DIRECT®
Biochemical and Biophysical Research Communications 314 (2004) 283–291
BBRC
www.elsevier.com/locate/ybbrc

siRNA-based inhibition specific for mutant SOD1 with single nucleotide alternation in familial ALS, compared with ribozyme and DNA enzyme☆,☆☆

Takanori Yokota,[a,c,*] Makoto Miyagishi,[b] Taro Hino,[a] Ryusuke Matsumura,[d] Tasinato Andrea,[c] Makoto Urushitani,[e] Rammohan V. Rao,[c] Ryosuke Takahashi,[e] Dale E. Bredesen,[c] Kazunari Taira,[b] and Hidehiro Mizusawa[a]

[a] *Department of Neurology, Tokyo Medical and Dental University, Tokyo, Japan*
[b] *Department of Chemistry and Biotechnology, The University of Tokyo, Tokyo, Japan*
[c] *The Laboratory of Genetics, The Buck Institute for Age Research, Novato, CA, USA*
[d] *Laboratory for Motor System, The Salk Institute for Biological Studies, San Diego, CA, USA*
[e] *Neurodegeneration, Brain Science Institute, RIKEN, Saitama, Japan*

Received 24 November 2003

Abstract

In many of autosomal dominant diseases such as familial amyotrophic lateral sclerosis (ALS) with SOD1 mutation, a missense point mutation may induce the disease by its gain of adverse property. Reduction of such a mutant protein expression is expected to improve the disease phenotype. Duplex of 21-nt RNA, known as siRNA, has recently emerged as a powerful tool to silence gene, but the sequence specificity and efficacies have not been fully studied in comparison with ribozyme and DNA enzyme. We could make the siRNA which recognized even a single nucleotide alternation and selectively suppress G93A SOD1 expression leaving wild-type SOD1 intact. In mammalian cells, the siRNA much more efficiently suppressed the expression of mutant SOD1 than ribozyme or DNA enzyme. Furthermore, these siRNAs could suppress cell death of Neuro2a induced by over-expression of mutant SOD1s with stress of proteasome inhibition. Our results support the feasibility of utilizing siRNA-based gene therapy of familial ALS with mutant SOD1.

Amyotrophic lateral sclerosis (ALS) is characterized by the degeneration of "lower motor neurons" in the spinal cord and brainstem, and degeneration of the descending motor pathway in the corticospinal tracts. Although most cases of ALS are sporadic and have an unknown etiology, 5–10% of ALS cases are familial, and of these, approximately 20% are due to missense, point mutations in the gene encoding Cu,Zn-superoxide dismutase (SOD1) [1]. Recent studies with transgenic mice and cell culture models of ALS with SOD1 mutations indicated that SOD1 mutations induce the disease by its toxic property, not by a loss of the SOD1 activity [2,3]. Similar 'gain of toxic function' of mutant protein is predicted to cause cell death in other autosomal dominant neurodegenerative diseases with a missense point mutation, such as familial Alzheimer's disease, prion disease, and Parkinson's disease. In all these familial diseases, one rational approach to therapy is to develop a method to specifically eliminate the aberrant protein.

RNA interference (RNAi) is the process of sequence-specific, post-transcriptional gene silencing, initiated by double-stranded RNA (dsRNA). This has a multi-step process that involves generation of 21–23 nt small interfering RNA (siRNA), resulting in degradation of the homologous RNA [4]. In mammalian cells, however, this provokes a strong cytotoxic response, leading to the

☆ *Abbreviations:* ALS, amyotrophic lateral sclerosis; SOD, superoxide dismutase; siRNA, small interfering RNA; dsRNA, double-stranded RNA; rAAVs, recombinant adeno-associated viruses.

☆☆ Supplementary data associated with this article can be found, in the online version, at doi:10.1016/j.bbrc.2003.12.098.

* Corresponding author. Fax: +81-3-5803-0169.
E-mail address: tak-yokota.nuro@tmd.ac.jp (T. Yokota).

0006-291X/$ - see front matter © 2003 Elsevier Inc. All rights reserved.
doi:10.1016/j.bbrc.2003.12.098

non-specific degradation of RNA transcripts and a general shut down of host cell protein translation [5,6]. This problem has been recently overcome by use of in vitro-synthesized siRNA, which is long enough to mediate gene-specific suppression, but short enough to evade adverse effects of long dsRNA [5].

Ribozymes and DNA enzyme are also small RNA/DNA molecules that possess sequence-specific RNA cleavage activity. Ribozymes occur naturally, but can also be created artificially to target specific sequences in *cis* or *trans* (i.e., on the same molecule or on a different molecule). They recognize and cleave a specific target sequence motif, 5′-NUX (where N is any nucleotide; X is A, C, or U) [7]. DNA enzyme or deoxyribozyme was derived by in vitro selection from a combinatorial library of DNA sequence and has a potential to cleave RNA at any purine (A, G)–pyrimidine (C, U) junction [8]. Both of ribozyme and DNA enzyme consist of a Mg^{2+}-dependent catalytic domain flanked by two substrate-binding arms and cleave a specific phosphodiester linkage of target RNA without recruiting endogenous nuclease. Ribozymes and DNA enzymes also can discriminate even a single nucleotide mismatch and have been successfully used to target and destroy specific RNAs. However, there was no report in which the specificity and efficiency of siRNA were directly compared with those of ribozyme and DNA enzyme.

In the present report, we have engineered siRNAs and DNA-based expressing siRNAs for mutant and wild-type SOD1s, to evaluate their efficiencies in comparison with ribozyme and DNA enzyme to decrease the expression of mutant SOD1 protein as a potential method for gene therapy of familial ALS.

Materials and methods

siRNA and DNA-vector based expressing siRNA preparation. The targeted region of siRNA was the coding sequence of SOD1 cDNA. The 5′ or 3′ UTRs and regions nearby the start codon are avoided, as these may be richer in regulatory protein binding sites. siRNA sequences of the form AA N_{19-20} and CA N_{19-20} with GC content less than 70% were selected from this region [9]. Next, the nucleotide preference after AA/CA is G or A, because it is required for efficient RNA polymerase initiation. Selected 19- or 20-nucleotide RNAs followed by TT or TdG were chemically synthesized and gel-purified. Synthesized single strand oligonucleotides were annealed at 95 °C for 1 min followed by slow cooling in the annealing buffer (PBS, pH 6.8, 2 mM $MgCl_2$).

siRNA-expressing vectors were made by modified reported methods using stem-loop type of siRNA [10,11]. The stem-loop type vector contains siRNA hairpin which contains 20–21 nt sense and antisense sequences of siRNA, connected by 3′ end of the sense strand and 5′ end of the antisense strand by a 9-nt loop sequence. Inserts containing the 9-nt loop sequence (TTCAAGAGA) flanked by sense and antisense siRNA sequences were made by PCR. These were inserted immediately downstream of U6 promotor in pUC19 [12].

Construction of plasmids encoding the substrate RNA and ribozymes. For target coding sequence cDNA clones of the human wild-type SOD1 and mutant A4V (kindly provided by T. Usdin) were used. Full-length human SOD1 cDNA was subcloned in the *Eco*RI and *Xba*I sites of pcDNA3 (Invitrogen). G93A, G93R, G93S, and G93C constructs were created using the QuikChange site-directed mutagenesis system from Stratagene. GFP–SOD1 fusion clones were constructed in *Eco*RI and *Sal*I sites of pEGFP-C2 (Clontech, Palo Alto, CA) using PCR method.

For a target site of hammerhead ribozyme, 5′-NUX (N = any nucleotide; X = A, U, or C) sequence [7] was selected. For the selection of DNA enzyme, purine–pyrimidine or AG [8] sequence was searched. DNA enzymes were chemically synthesized. Ribozyme coding sequences were made from two complementary synthetic DNA oligonucleotides flanked by *Xba*I and *Eco*RI restriction sites. These oligonucleotides were annealed and ligated into pcDNA3(−) (Invitrogen). Each ribozyme was followed by internally cleaving hairpin ribozyme [13].

Cell culture and transfection. Cells from the human embryonic kidney cell line 293T (293T) and mouse Neuro2a were cultured in Dulbecco's modified Eagle's medium containing 10% fetal bovine serum with 1% penicillin/streptomycin. Transient transfection using Lipofectamine Plus reagent (Life Technologies, Rockville, MD) was carried out in 24-well plates with cells reaching 40–60% confluence. Mutant or wild-type SOD1 expression plasmid (0.25 μg) and 2.5–125 nM (0.07–3.5 μg) siRNA, 0.5–2.0 μg DNA-vector-based expressing siRNAs, 10 μg DNA enzyme, or 1.0–2.0 μg ribozyme expression plasmid were transfected together with 0.05 μg GFP expression plasmid (pEGFP-C2; Clontech) to monitor for transfection efficiency. The medium for DNA enzyme was changed with fresh medium containing 1 μg DNA enzyme at 24 h after transfection. For control transfection of the same volume of siRNA, DNA enzyme for unrelated Machado-Joseph disease gene or empty pcDNA3 was used.

For fluorescence analysis, 0.25 μg GFP fused-mutant or wild-type SOD1 expression plasmids and 25 nM siRNA were transfected with 0.1 μg DsRed expression vector (pDsRed2; Clontech) to monitor for transfection efficiency. Cell was visualized with fluorescence microscopy (Nikon, Tokyo).

In vitro transcription and cleavage reactions by ribozyme and DNA enzyme. Plasmids containing target SOD1 sequences were linearized with *Xba*I, and plasmids containing ribozyme sequences with *Eco*RI. In vitro transcription was performed with 10 μg linear DNA template and T7 RNA polymerase using RiboMAX (Promega) and labeled by incorporation of [α-^{32}P]uridine triphosphate. After digesting DNA with DNase I, the transcripts were purified.

For standard cleavage reactions in vitro, 8 μM SOD1 substrate RNA and 40 μM ribozyme or 40 μM DNA enzyme were mixed in a 10 μl reaction buffer containing 20 mM $MgCl_2$ and 40 mM Tris–HCl (pH 7.5). The mixture was incubated at 37 °C for 1–4 h and stopped by addition of 50 mM EDTA, and then an equal volume of 10 M urea and 0.02% bromphenol blue. The cleavage products were denatured at 90 °C for 2 min and electrophoresed in 6% polyacrylamide–7 M urea gel in Tris–borate EDTA buffer.

Western blot analysis. At 24 or 48 h after transfection, cells were harvested by gentle scraping in lysis buffer (50 mM Tris–HCl, 150 mM NaCl, 1% Triton X, and a proteinase inhibitor cocktail, Complete (Roche)). Equal amounts of total cellular protein were mixed with 5× Laemmli sample buffer, denatured at 95 °C for 5 min, and separated on 15% SDS–polyacrylamide gels. Protein was transferred electrophoretically to polyvinylidene difluoride membranes, immunoblotted with anti-SOD1 polyclonal antibody S-100 (Stressgen Biotechnologies) and anti-GFP monoclonal antibody (Clontech), and detected using enhanced chemiluminescence (Amersham–Pharmacia Biotech).

All experiments of Western blotting were separately performed at least three times.

Cell-toxicity assay. Neuro2a cells in 24-well culture plates were co-transfected with mutant or wild-type SOD1 expression plasmid (1.0 μg/well), 25 nM siRNA (or 1.0 μg expressing siRNA vector), and pCMV-β-gal (50 ng/well) (Clontech). The medium was replaced with that containing 2 mM dibutyryl cyclic-AMP 3 h after transfection to

differentiate the cells. At 24 h after transfection, proteasome inhibitor, lactacystin (20 μM), was added to the medium. At 48 h, the cells were harvested and assayed with β-galactosidase assay kit (Promega). The LacZ expression levels correlate with cellular viability [14]. The percent viability was calculated in comparison with control lysates without lactacystin. Statistical significance was evaluated by single factor ANOVA (analysis of variance) or two-way ANOVA followed by Scheffe's method.

Results

Suppression effect of siRNA, DNA enzyme, and ribozyme specific for mutant SOD1 at codon 93

siRNA and expressing siRNA for G93A SOD1

Two siRNAs targeting G93A SOD1 corresponding to regions 277–297 (siRNA G93A.1) and 275–294 (siRNA G93A.2) were designed (Fig. 1A). Transfection of both siRNAs into mammalian cells could effectively reduce G93A SOD1 expression. Western blot analysis revealed that both siRNA G93A.1 and 2 reduced the expression of G93A SOD1 protein by about 90% when expression efficiency was adjusted with co-transfected GFP (Fig. 1B). The suppression of G93A SOD1 protein by siRNA G93A.1 increased in a dose-dependent manner when the amount of siRNA was changed from 2.5 to 125 nM (Fig. 1C). These siRNAs recognized only one nucleotide alteration, because they suppressed wild-type SOD1 protein much less than G93A SOD1—especially siRNA G93A.2, for which the reduction of wild type was only 1.8% (Fig. 1B). These suppression effects were confirmed by the reduction in GFP fluorescence when siRNA was co-transfected with a GFP-fused SOD1 plasmid (Fig. 1D) using DsRed fluorescence as a control for transfection efficiency (data not shown).

All these results were similarly confirmed in both 293T and Neuro2a cells.

DNA enzyme and ribozyme

We can design the G93A-specific DNA enzyme (Dz G93A) which cleaves G93A mutant SOD1 RNA, but not wild-type SOD1 RNA. Because the wild-type purine-purine sequence at G93A site (GGT) that is not recognized by the DNA enzyme is mutated to a

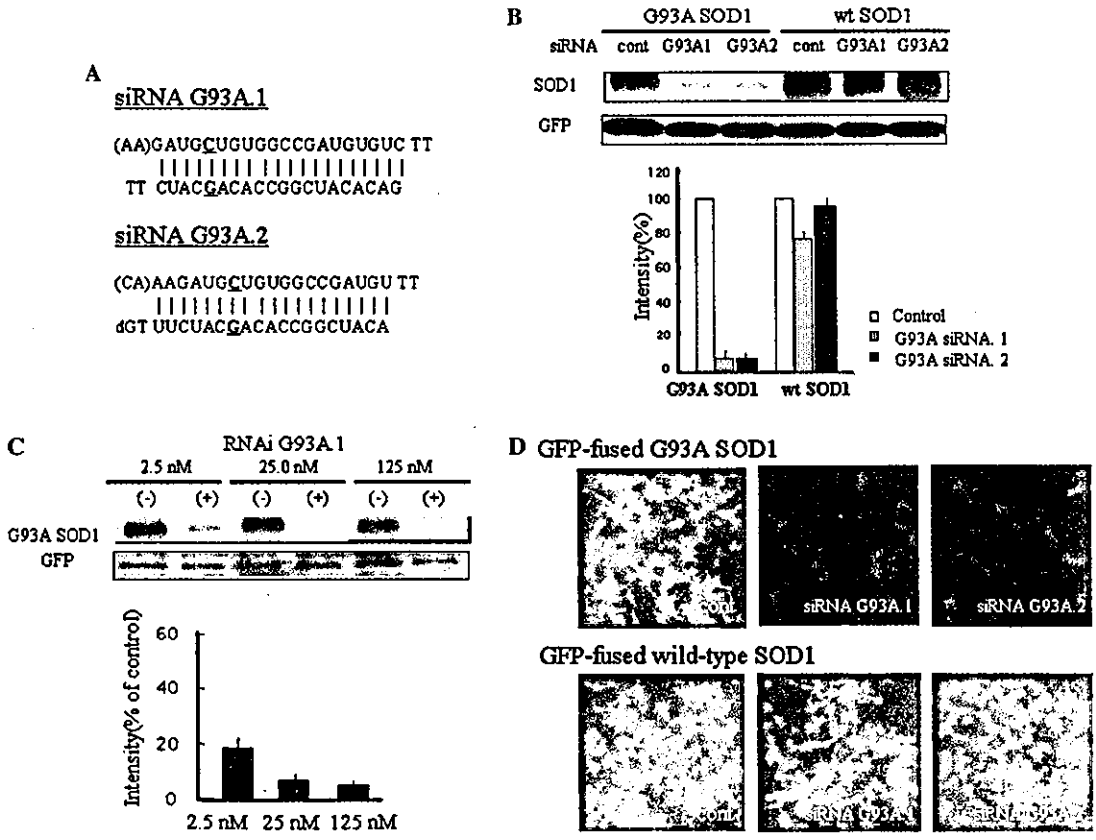

Fig. 1. siRNAs specific for G93A SOD1. (A) Sequences of siRNA G93A.1 and G93A.2. Underlined characters indicate mutations. (B) Effect of siRNA G93A.1 and 2 on G93A and wild-type SOD1 proteins (with no tag) expressed in 293T cells as detected by Western blotting with anti-SOD1 antibody. Expression level of target protein was adjusted by level of co-transfected GFP expression (B). Data are at 48 h after transfections. (C) Dose-dependent effect of suppression of siRNA G93A.1. Figure shows the percentages of band intensity with siRNA G93A.1 with respect to that with each mock transfection. (D) Effect of siRNA G93A.1 and 2 on fluorescence of GFP-fused SOD1s. Expression level of target protein was adjusted by level of co-transfected DsRed fluorescence (data not shown). Values are means and SEM.

purine-pyrimidine (GCT) sequence that is cleaved by the DNA enzyme. The sequence of Dz G93A is shown in Fig. 2A. Cleavage of SOD1 mRNA was carried out by incubating in vitro transcribed mRNA with Dz G93A. The cleavage by Dz G93A resulted in two discrete products from G93A SOD1 mRNA in a sequence-specific manner (Fig. 2B, left). In contrast, Dz G93A produced no detectable cleavage of wild-type target mRNA. Because of the key role of Mg^{2+} in RNA structure and in the cleavage of phosphodiester bonds, cleavage of the mutant was also assessed in the absence of $MgCl_2$ and no cleavage was observed. Next, in order to optimize the arm length to get the most effective cleavage, it was varied from 6 to 12 bases. The maximum cleavage effect was observed when the arm length was 9 bases (Fig. 2B, right). For stabilization of DNA enzyme to degradation by DNAase in cells, the two nucleotides of DNA enzymes were modified with phosphorothioate at both their 5′ and 3′ ends. This modified Dz G93A was confirmed to remain active and specific for mutant mRNA in an in vitro cleavage assay (supplement figure).

For the design of ribozyme, G93A sequence at the mutation site does not follow NUX rule, but sequences of other reported mutations at the same codon, G93R, G93S, and G93C [15], can be targeted by ribozyme. AUX triplet of G93R, G93S, and G93C is cleaved by Rz G93X, but the corresponding triplet in the wild-type, AUG, does not follow the NUX rule (Fig. 2A). The sequences of Rz G93R, G93S, and G93C are shown in Fig. 2A. In vitro cleavage reactions demonstrated that Rz G93X could convert G93R, G93S, and G93C mRNAs to the expected two cleavage products, but that wild-type mRNA was, as expected, resistant to cleavage (Fig. 2C). The optimal arm length of Rz G93X was proved to be 8 for the maximum effect (data not shown).

Rz G93X or phosphorothioate-modified Dz G93A was co-transfected with plasmids encoding each mutant SOD1 to investigate their suppression effect of protein in

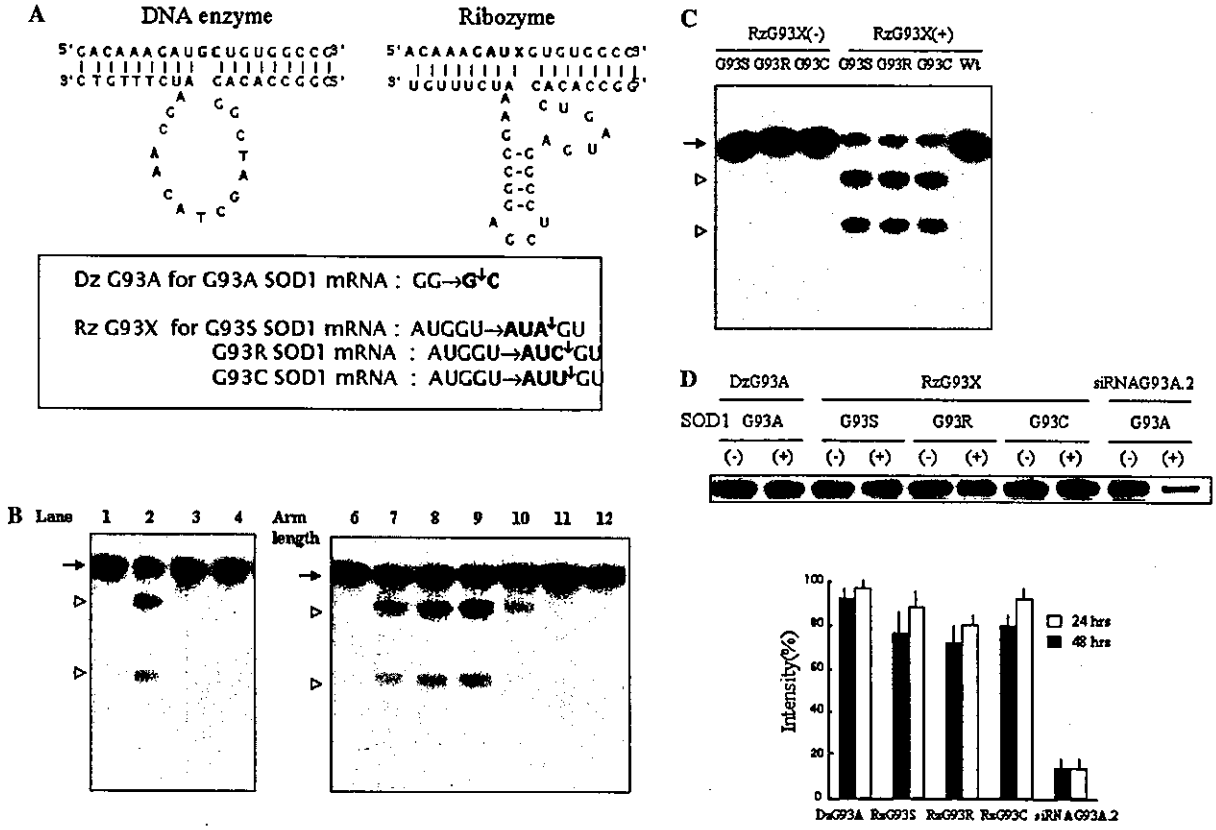

Fig. 2. DNA enzyme and ribozyme specific for mutant SOD1 at codon 93. (A) Sequences of DNA enzyme and ribozyme (upper panel) and target sequence of wild-type and mutant SOD1s. Bold characters are the target sequences. Vertical arrows indicate cleavage sites. (B) Sequence-specific (left) and arm length-dependent (right) cleavage of G93ASOD1 mRNA by Dz G93A. When [α-^{32}P]-labeled G93ASOD1 RNAs were incubated with unlabeled Dz G93A in buffer with 20 mM Mg^{2+} for 4 h, the target RNA was cleaved into two expected products in 4 h (lane 2) (lane 1, before reaction), but was not cleaved without Mg^{2+} in the reactions (lane 3). Dz G93A did not cleave wild-type SOD1 mRNA (lane 4). Cleavage by DzG93A was most effective when the arm length was nine nucleotides (right panel). Arrow, full-length SOD1 mRNA (765 nt); arrowheads, fragments (581 and 184 nt). (C) Sequence-specific cleavage of mutant SOD1 mRNAs by RzG93X in vitro. [α-^{32}P]-Labeled G93S, G93R, and G93C mRNAs were incubated with unlabeled Rz G93X for 4 h. RzG93X could cleave all three mutant mRNAs, but not wild-type mRNA. Arrow, full-length SOD1 mRNA (765 nt); arrowheads, fragments (581 and 184 nt). (D) Western blot analysis of the effect of Rz G93X, Dx G93A, and siRNA G93A on the expression of mutant SOD1 proteins in 293T cells. Blot is from 48 h after transfection. Figure shows the percentages of band intensity with Rz G93X, Dx G93A, and siRNA G93A (+) with respect to those with mock transfection (−). Values are means and SEM.

mammalian cells. The DNA enzyme at 1–10 μg had very little effect and 2 μg ribozymes suppressed expression of each mutant only to the extent of 30% in 24 h. In contrast, 2.5 nM siRNA G93A.2 (= 0.07 μg) suppressed the expression of G93A SOD1 by more than 80% as reflected in the band intensity on Western blotting both at 24 and 48 h after transfection (Fig. 2D). Thus, on a molarity comparison basis, siRNA was more effective than either ribozyme or DNA enzyme in suppressing mutant SOD1 expression.

Suppression effect of siRNA, DNA enzyme, and ribozyme for wild-type SOD1

Four siRNAs for wild-type SOD1 were designed (Fig. 3A). These siRNAs were named by the nucleotide number at the center position of each siRNA sequence towards the 5′ side of which the siRNA is presumed to cleave the substrate RNA [8,9]. siRNA396 most effectively suppressed SOD1 expression in 293T (Fig. 3B, upper) and Neuro2a cells (data not shown). In addition, this siRNA396 could suppress the expression of any mutant SOD1, such as G93A, A4V (Fig. 3B, lower), G85R or G93S (data not shown) with a similar degree of efficiency as wild-type SOD1. siRNA396 could reduce the expression of endogenous human SOD1 in 293T cells (Fig. 3C) and mouse SOD1 in N2a cells (data not shown). This reduction was most prominent at 24 h and expression returned to the normal level in 96 h.

For comparing the efficacy of siRNA, DNA enzymes, and ribozymes for wild-type SOD1, they were designed from the region between nucleotide number 382 and 419 of SOD1 ORF mRNA. The 382–419 region is presumed to be the biggest single-strand RNA region with minimal free energy (Fig. 4A, arrow), when the secondary structure of SOD1 mRNA is analyzed with the mFold program of Zuker (http://mfold.wustl.edu/~folder/rna/form1.cgi). Two siRNAs, siRNA396 and 412, three DNA enzymes, Dz394, Dz398, and Dz403, and one ribozyme, Rz405, were designed within this region (Fig. 4A). DNA enzyme and ribozyme were named by the nucleotide number on the 5′ side of the cleavage site. An in vitro cleavage assay revealed that more than 90% of the full-length mRNA was converted to the expected products by Dz394 and Rz405 after 4 h of incubation (Fig. 4B). However, in 293T and Neuro2a cells, Dz394 did not suppress the expression of SOD1 protein and Rz405 suppressed only about half of the expression. In contrast, siRNA396 suppressed the expression almost to the baseline level (Fig. 4C). As to any suppression effect on endogenous SOD1 of 293T cells, neither DNA enzyme nor ribozyme decreased the endogenous expression clearly (Fig. 4D).

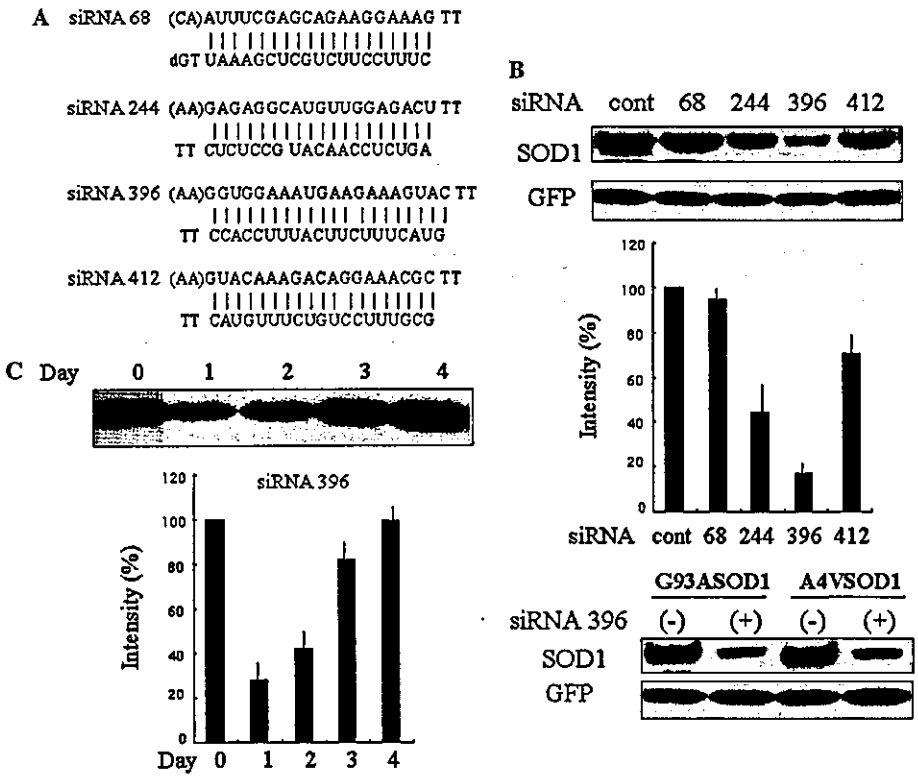

Fig. 3. siRNAs for wild-type SOD1. (A) Sequences of four siRNAs for wild-type SOD1. (B) Effect of four non-specific siRNAs on wild-type SOD1(with no tag) (upper panel) and mutant SOD1(with no tag) (lower panel) expressions in 293T cells as detected by Western blotting with anti-SOD1 antibody. Expression level of target protein was adjusted by level of co-transfected GFP expression. (C) Western blot analysis of the effect of siRNA 396 on endogenous wild-type SOD1 in 293T cells. Values are means and SEM.

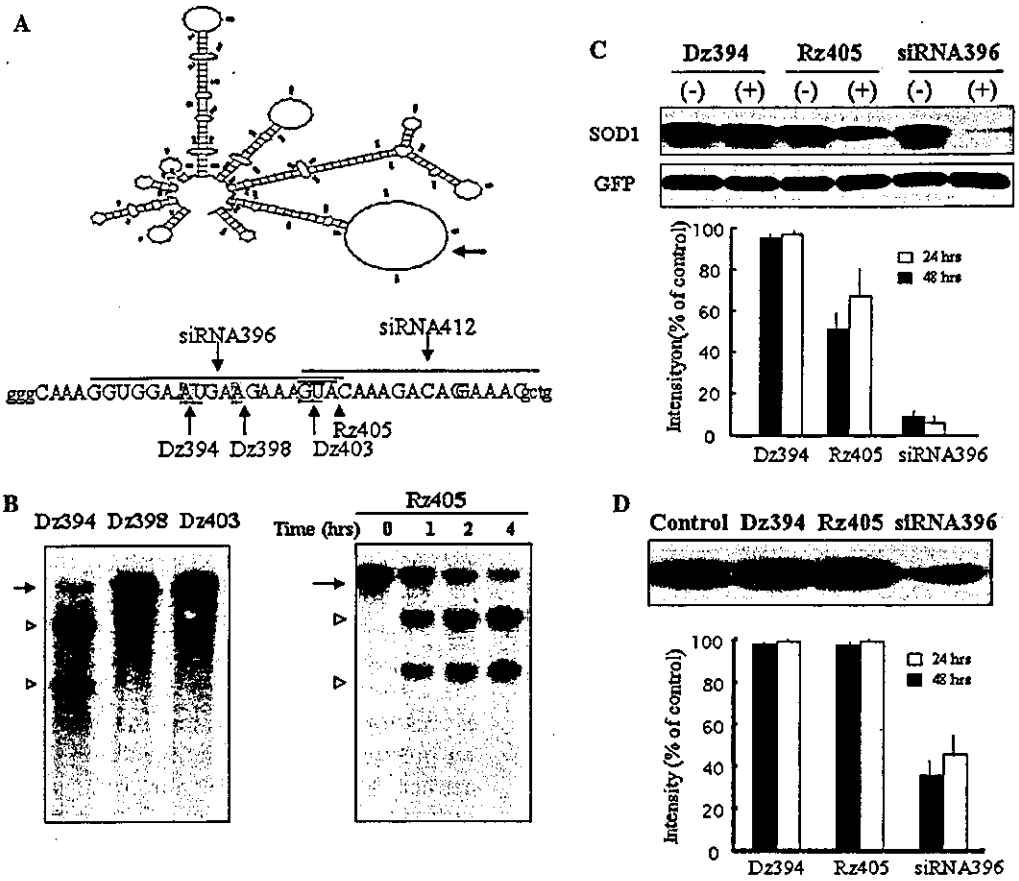

Fig. 4. DNA enzyme, ribozyme, and siRNA targeting predicted single-strand region 382–419 of wild-type SOD1 mRNA. (A) Secondary structure of the coding region of human SOD1 mRNA (upper panel). Arrow indicates the largest single-strand region (382–419) with minimal free energy. Locations of candidate cleavage site of DNA enzyme, ribozyme, and siRNA within region of 382–419 (lower panel). Upper-case letters of 382–419 sequences are included in the single-strand region and lower-case letters are in the stem region. (B) Sequence-specific cleavage of DNA enzymes (left) and Rz 405 (right). [α-^{32}P]-Labeled wild-type SOD1 RNA was incubated with DNA enzymes for 4 h. Dz 394 cleaved most of the target RNA into the two expected products, but other DNA enzymes did not (left). Arrow, full-length SOD1 mRNA (765 nt); arrowheads, fragments (446 and 319 nt). Rz 405 cleaved most of the target RNA in a time-dependent manner (right). Arrow, full-length SOD1 mRNA (765 nt); arrowheads, fragments (457 and 308 nt). (C) Effect of Dz394, Rz405, and siRNA396 on wild-type SOD1 proteins (with no tag) expressed in 293T cells as detected by Western blotting with anti-SOD1 antibody. Expression level of target protein was adjusted by level of co-transfected GFP expression. (D) Western blot analysis of the effect of siRNA 396 on endogenous wild-type SOD1 in 293T cells. Values are means and SEM.

DNA-vector based expressing siRNA

The 0.5 and 2.0 μg of DNA-vector based expressing siRNAs were co-transfected with 0.25 μg of wild-type or mutant SOD1-containing plasmids in 293T and Neuro2a cells. Both expressing siRNA vectors for G93A, siRNA V. G93A.1 and 2, significantly suppressed expression of G93ASOD1 protein, and the suppression ratios were comparable to those by siRNA G93A.1 and 2 of oligonucleotide with very little effect on wild-type SOD1 expression (Fig. 5A). There was not much difference in efficiency between 0.5 and 2.5 μg of expressing siRNAs (data not shown). The expressing siRNA vector for wild-type SOD1, siRNA V. 396, could inhibit markedly the expressions of wild-type, G93A, and A4V SOD1 proteins in similar degrees to siRNA 396 of oligonucleotide (Fig. 5B). The siRNA V. 396 suppressed the endogenous human SOD1 in 293T cells (Fig. 5C) and mouse SOD1 in N2a cells (data not shown).

Cell-toxicity assay

The suppressive effect of siRNA on mutant-SOD1-induced cell toxicity was tested using Neuro2a cells. The survival rates of mutant transformants were significantly decreased compared with wild-type transformant and vector controls in the presence of lactacystin, a proteasome inhibitor. siRNA G93A.2 increased the survival rate of G93A, but not that of A4V transformant. In contrast, siRNA396 increased the survival rates of both G93A and A4V transformants (Fig. 6). Similar effects were observed with transfection of siRNA V.G93A.2 and 396 (data not shown).

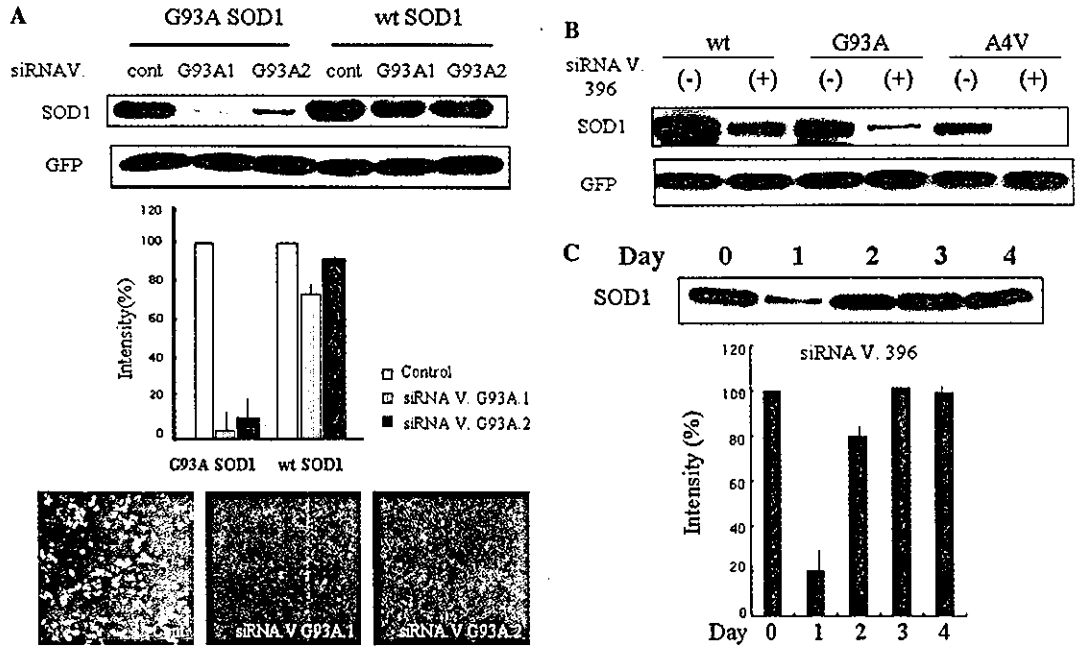

Fig. 5. Effect of DNA-vector based expressing siRNAs (siRNA V.). (A) Effect of expressing siRNA vectors for G93A SOD1 (siRNA V. G93A.1 and 2) on G93A and wild-type SOD1 protein (with no tag) expressed in Neuro2a cells as detected by Western blotting with anti-SOD1 antibody. Expression level of target protein was adjusted by level of co-transfected GFP expression (upper panel). Fluorescence of GFP-fused SODs was also suppressed by siRNA V. G93A.1 and 2 (lower panel). Expression level of target protein was adjusted by level of co-transfected DsRed fluorescence (data not shown). Data are at 48 h after transfections. Values in the figure are means and SEM. (B) Effect of expressing siRNA vectors for wild-type SOD1 (siRNA V.394) on wild-type, G93A, and A4V SOD1 protein (with no tag) expressed in 293T cells as detected by Western blotting with anti-SOD1 antibody. Expression level of target protein was adjusted by level of co-transfected GFP expression. (C) Western blot analysis of effect of siRNA V.396 on endogenous wild-type SOD1 expression in 293T cells. Values are means and SEM.

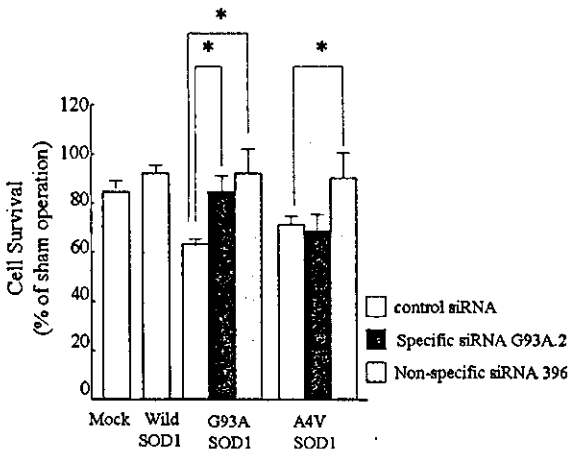

Fig. 6. siRNAs rescue the mutant SOD1-induced toxicity in mammalian cells. The relative viability of the wild-type, mutant, and mock transfectants treated with lactacystin (20 μM) compared with each without treatment of lactacystin. Lactacystin enhances the mutant SOD1-related toxicity in Neuro2a cells. siRNA G93A.2 increased the viability of G93A SOD1-transformant to the similar level of mock-transformant, but did not improve that of A4V SOD1-transformant. siRNA 396 increased the viabilities of both G93A and A4V SOD1-transformants. Values are means and SEM.

Discussion

In autosomal dominant disease, such as familial ALS, the most effective therapeutic approach requires the reduction of the aberrant mutant protein leaving wild-type protein intact. Possible candidate methods include ribozyme, DNA enzyme, and siRNA to cleave mutant RNA selectively. Antisense RNA or DNA has been used to reduce the expression of target protein, but these do not discriminate between the wild-type and mutant mRNA of SOD1, most of which has a point mutation [15]. siRNA G93A.1 and 2, which were designed to target the G93A mutant specifically, suppressed the expression of approximately 90% of G93A SOD1 protein, a suppression rate that is similar to that described in the original report on siRNA [5]. In contrast, they had much less effect on the expression of wild-type SOD1 and especially siRNA G93A.2 had close to no effect on wild-type SOD1 expression. While nucleotides in the 3′- and 5′- terminal region (except for the 3′ overhang of the siRNA sequence) do not contribute to the specificity of target recognition, nucleotides in the center of the siRNA sequence are important specificity determinants [5,16]. That the mutation site in siRNA G93A.2 is located more in the center of the sequence than that in siRNA G93A.1 might explain the lesser effect of G93A.2 on wild-type SOD1 compared to G93A.1.

Ribozymes and DNA enzymes also can discriminate even a single nucleotide mismatch. In our experiments the ribozyme and DNA enzyme, designed for SOD1 mutants at codon 93, were absolutely specific for the mutant

sequence, as shown by in vitro cleavage reactions. However, in contrast to the specificity, suppression of mutant SOD1 protein expression by them in the mammalian cells was much lower than that obtained with siRNA G93A under the conditions used in our investigation.

Two possible explanations may account for such a big difference in efficiency between siRNA and DNA enzyme/ribozyme at codon 93. First, double-stranded siRNAs are protected by proteins in cells from attacks by ribonucleases, whereas single-stranded RNA/DNA are not, as demonstrated earlier [11]. Second, the secondary structure of SOD1 mRNA at this site might not be accessible by ribozyme or DNA enzyme. The secondary structure of target RNA highly influences the efficiencies of ribozyme and DNA enzyme, but not that of siRNA [4,5,16], probably because, in some step of siRNA, ATP-dependent RNA helicase may unwind duplex RNA [9,17]. Therefore, we also compared the ribozyme, DNA enzyme, and siRNA that were designed to target the largest single-strand region of SOD1 ORF mRNA with minimal free energy predicted by the mFold program of Zuker. Actually, Rz405 and Dz398 cleaved most of the in vitro-transcribed full-length SOD1 RNA in 4 h, with efficiencies that were much better than those for Rz G93X and Dz G93A, and were comparable to or even better than those of reported constructs [18,19]. For the ribozyme expression in the cells, furthermore, an internally cleaved hairpin ribozyme cassette was inserted downstream of the hammerhead ribozyme to remove 3′ extraneous sequences, which may interfere with ribozyme activity [13,20]. Rz405, as well as Dz398 was, however, still much less efficient in the cells than siRNA396.

It is a very important result for the gene therapy of congenital disease that siRNA396 could efficiently suppress endogenous SOD1 expression. Considering the facts that the half-life of SOD1 protein is a few days and that transfection efficiency of siRNA was 80–90% (judging by the result of the control GFP plasmid), a 60–70% reduction of total endogenous SOD1 by siRNA396 (Fig. 3C) suggests nearly complete elimination of endogenous SOD1 expression in the successfully transfected cells. In contrast, neither Rz405 nor Dz398 was effective in suppressing endogenous SOD1 expression. Therefore, the current studies would suggest that siRNA is clearly a potent and promising tool for silencing of the target gene in cells.

Although our non-specific siRNAs do not discriminate between mutant and wild-type SOD1 mRNAs, it is possible that a reduction in expression of both mutant and wild-type SOD1 may also be beneficial for rescue of the phenotype. There are several lines of evidences suggesting that reduction of wild-type SOD1 activity will not produce or enhance the phenotype of motor neuron loss. First, in ALS patients with SOD1 mutations neither the age of onset nor the rapidity of progression of disease correlates with SOD1 activity level [15]. Although the downregulation of SOD1 may cause neuronal death in cultured cells [21], SOD1 null mice developed normally without motor neuron disease [22]. More importantly, elimination of wild-type endogenous SOD1 by crossing G85R SOD1 transgenic mice with SOD1 null mice was found to have no effect on mutant-mediated disease [23]. These observations suggest the possibility that reduction of mutant proteins, even if it is accompanied by the reduction of wild-type SOD1 to a similar degree, may be sufficient for improving the phenotype. In our cell line model, indeed, siRNA396, which suppressed expression of both mutant and wild-type SOD1, rescued the enhanced cell toxicity produced by overexpression of G93A and A4V SOD1s.

For the application of the siRNA approach to gene therapy of neurodegenerative disease in vivo, we must develop a way to achieve long-term expression of siRNA in post-mitotic neurons (and possibly glia, as well). siRNA therapy, like antisense DNA and DNA enzyme therapies, requires continuous delivery of sufficient quantities of therapeutic molecules to inhibit translation of target mRNA. In contrast, ribozyme encoded in recombinant adeno-associated viruses (rAAVs) can be incorporated in the host chromosomal DNA in neurons and transcribed indefinitely [24]. Therefore, in order to use a viral delivery system for siRNA, we tried vector-mediated expression of siRNA. We constructed a DNA-based siRNA expression vector in which each sense and antisense siRNA sequence was placed under control of human U6 promoter with a termination signal at the 3′ end (short stretch of uridines). Expressed stem-loop transcript would be cleaved by endogenous Dicer and form siRNA duplexes with two 3′ overhangs in the cells. All of the expressing vectors of siRNA G93A.1, G93A.2, and 396 worked well, i.e., to the similar degree to siRNA of oligonucleotides in cells. We are in the process of making rAAV and transgenic mice expressing siRNA396 and G93A.2 for investigating the efficacy of siRNAs in vivo. Although a less-invasive delivery method for introducing in vivo cells is needed for clinical feasibility, the efficiency of our siRNA and expressing RNA vector to reduce mutant SOD1 protein in cells suggests that this mRNA-targeting approach by siRNA might provide effective therapy for autosomal dominant disease, such as familial ALS.

Acknowledgments

The authors thank Alyson Peel, Ph.D., Dr. Li Yi, Dr. Hiroki Sasaguri, and Dr. Yuki Saito for their help. This study was supported by Grants from the National Institutes of Health (NS35155 to D.E.B.) and the ALS Association, the Ministry of Education, Science and Culture, Japan (A-130, T.Y.), from the Ministry of Health, Labor and Welfare, Japan (T.Y., H.M.), and from Japan Amyotrophic Lateral Sclerosis Association (T.Y.).

References

[1] D.R. Rosen, T. Siddique, D. Patterson, D.A. Figlewicz, P. Sapp, A. Hentati, D. Donaldson, J. Goto, J.P. O'Regan, H.X. Deng, Mutations in Cu, Zn superoxide dismutase are associated with familial amyotrophic lateral sclerosis, Nature 362 (1993) 59–66.

[2] D.W. Cleveland, From Charcot to SOD1: mechanisms of selective motor neuron death in ALS, Neuron 24 (1983) 515–520.

[3] C. Baglioni, T.W. Nilsen, Mechanisms of antiviral action of interferon, Interferon 5 (1999) 23–42.

[4] B.R. Williams, Role of the double-stranded RNA-activated protein kinase (PKR) in cell regulation, Biochem. Soc. Trans. 25 (1997) 509–513.

[5] S.M. Elbashir, J. Harborth, W. Lendeckel, A. Yalcin, K. Weber, T. Tuschl, Duplexes of 21-nucleotide RNAs mediate RNA interference in cultured mammalian cells, Nature 411 (2001) 494–498.

[6] S.M. Elbashir, J. Martinez, A. Patkaniowska, W. Lendeckel, T. Tuschl, Functional anatomy of siRNAs for mediating efficient RNAi in *Drosophila melanogaster* embryo lysate, EMBO J. 20 (2001) 6877–6888.

[7] D.E. Ruffer, G.D. Stormo, O.C. Uhlenbeck, The sequence requirements of the hammerhead self-cleavage reaction, Biochemistry 29 (1990) 10695–10702.

[8] S.W. Santoro, G.F. Joyce, A general purpose RNA-cleaving DNA enzyme, Proc. Natl. Acad. Sci. USA 94 (1997) 4262–4266.

[9] P.A. Sharp, RNA interference, Genes Dev. 15 (2001) 485–490.

[10] T.R. Brummelkamp, R. Bernards, R. Agami, A system for stable expression of short interfering RNAs in mammalian cells, Science 296 (2002) 550–553.

[11] M. Miyagishi, K. Taira, U6 promotor-driven siRNAs with four urideine 3′ overhangs efficiently suppress targeted gene expression in mammalian cells, Nat. Biotechnol. 19 (2002) 497–500.

[12] J. Ohkawa, K. Taira, Control of the functional activity of an antisense RNA by a tetracycline-responsive derivative of the human U6 snRNA promoter, Hum. Gene Ther. 11 (2000) 577–585.

[13] M. Altschuler, R. Tritz, A. Hampel, A method for generating transcripts with defined 5′ and 3′ termini by autolytic processing, Gene 122 (1992) 85–90.

[14] H.B. Oral, C.V. Arancibia-Carcamo, D.O. Haskard, A.J. George, A method for determining the cytoprotective effect of catalase in transiently transfected cell lines and in corneal tissue, Anal. Biochem. 267 (1999) 196–202.

[15] A. Radunovic, P.N. Leigh, Cu/Zn superoxide dismutase gene mutations in amyotrophic lateral sclerosis: correlation between genotype and clinical features, J. Neurol. Neurosurg. Psychiatry 61 (1996) 565–572.

[16] T. Holen, M. Amarzguioui, M. Wiiger, E. Babaie, H. Prydz, Positional effects of short interfering RNAs targeting the human coagulation trigger tissue factor, Nucleic Acids Res. 30 (2002) 1757–1766.

[17] T. Dalmay, R. Horsefield, T.H. Braunstein, D.C. Baulcombe, SDE3 encodes an RNA helicase required for post-transcriptional gene silencing in *Arabidopsis*, EMBO J. 20 (2001) 2069–2078.

[18] M. Warashina, T. Kuwabara, Y. Nakamatsu, K. Taira, Extremely high and specific activity of DNA enzymes in cells with a Philadelphia chromosome, Chem. Biol. 6 (1999) 237–250.

[19] F.S. Santiago, H.C. Lowe, M.M. Kavurma, C.N. Chesterman, A. Baker, D.G. Atkins, L.M. Khachigian, New DNA enzyme targeting Egr-1 mRNA inhibits vascular smooth muscle proliferation and regrowth after injury, Nat. Med. 5 (1999) 1264–1269.

[20] J. Ohkawa, N. Yuyama, Y. Takebe, S. Nishikawa, K. Taira, Importance of independence in ribozyme reactions: kinetic behavior of trimmed and of simply connected multiple ribozymes with potential activity against human immunodeficiency virus, Proc. Natl. Acad. Sci. USA 90 (1993) 11302–11306.

[21] J.D. Rothstein, L.A. Bristrol, B. Hosler, R.H. Brown, R.W. Kuncl, Chronic inhibition of superoxide dismutase produces apoptotic death of spinal neurons, Proc. Natl. Acad. Sci. USA 91 (1994) 4155–4159.

[22] A.G. Reaume, J.L. Elliott, E.K. Hoffman, N.W. Kowall, R.J. Ferrante, D.F. Siwek, H.M. Wilcox, D.G. Flood, M.F. Beal, R.H. Brown Jr., Motor neurons in Cu/Zn superoxide dismutase-deficient mice develop normally but exhibit enhanced cell death after axonal injury, Nat. Genet. 13 (1996) 43–47.

[23] L.I. Bruijn, M.K. Houseweart, S. Kato, K.L. Anderson, S.D. Anderson, E. Ohama, A.G. Reaume, R.W. Scott, D.W. Cleveland, Aggregation and motor neuron toxicity of an ALS-linked SOD1 mutant independent from wild-type SOD1, Science 281 (1998) 1851–1854.

[24] A.S. Lewin, K.A. Drenser, W.W. Hauswirth, S. Nishikawa, D. Yasumura, J.G. Flannery, M.M. LaVail, Ribozyme rescue of photoreceptor cells in a transgenic rat model of autosomal dominant retinitis pigmentosa, Nat. Med. 4 (1998) 967–971.

Sequence-Dependent and Independent Inhibition Specific for Mutant Ataxin-3 by Small Interfering RNA

Yi Li, MD,[1] Takanori Yokota, MD,[1]
Ryusuke Matsumura, MD,[2] Kazunari Taira, PhD,[3]
and Hidehiro Mizusawa, MD[1]

In Machado–Joseph disease (MJD) gene, there is a C/G polymorphism immediately after the CAG repeat; the expanded CAG repeat tract is exclusively followed by C, whereas about half of wild-type alleles are followed by G. Using this C/G polymorphism, we have engineered the small interfering RNA (siRNA) which decreased the expression of mutant ataxin-3, Q79C, by 96.0%, whereas there was minimal reduction on that of the wild type, Q22G (5.9%). Furthermore, unexpectedly, the expression of another wild-type allele, Q22C, was also much less suppressed (22.5%) by this siRNA possibly due to difference of the secondary structure of the target RNA. This is the first report of sequence-independent discrimination of mutant and wild-type alleles by siRNA.

Ann Neurol 2004;56:124–129

From the [1]Department of Neurology and Neurological Science, Graduate School, Tokyo Medical and Dental University, Tokyo; [2]Department of Neurology, Nara Medical University, Nara; [3]Department of Chemistry and Biotechnology, School of Engineering, University of Tokyo, Tokyo, Japan.

Received Nov 24, 2003, and in revised form Feb 25, 2004. Accepted for publication Apr 2, 2004.

Published online Jun 28, 2004, in Wiley InterScience (www.interscience.wiley.com). DOI: 10.1002/ana.20141

Address correspondence to Dr Yokota, Department of Neurology, Tokyo Medical and Dental University, 1-5-45 Yushima, Bunkyo-ku, Tokyo 113-8519, Japan. E-mail: tak-yokota.nuro@tmd.ac.jp

Machado–Joseph disease (MJD) is an autosomal dominant neurodegenerative disorder that is characterized clinically by cerebellar ataxia, pyramidal and extrapyramidal signs, peripheral neuropathy, and ophthalmoplegia. The number of CAG in MJD1 gene repeats is between 13 and 36, whereas in patients this range is expanded from 62 to 84.[1] The pathogenosis of MJD is considered to be caused by "gain of toxic function" of mutant MJD protein.[2,3] Therefore, a most effective and simple gene therapeutic approach for MJD requires the reduction of the aberrant mutant protein. Furthermore, it might be needed to reduce mutant ataxin-3 selectively, leaving wild-type protein intact, because the wild-type MJD1 gene product ataxin-3 should have an important role in cell survival, such as quality control of endoplasmic reticulum[4] and DNA repair.[5]

RNA interference (RNAi) is the process of sequence-specific, posttranscriptional gene silencing, initiated by double-stranded RNA (dsRNA). This has a multistep process that involves the generation of 21 to 23-nucleotide small interfering RNA (siRNA), resulting in degradation of the homologous RNA. The siRNA is long enough to mediate gene-specific suppression but short enough to evade adverse effects of long dsRNA in mammalian cells[6] and is expected to be a powerful tool for gene therapy of human diseases.

We found that the CAG repeat tract in the MJD1 gene is followed by C or G and there is extreme bias of this C/G polymorphism between mutant and normal MJD1 alleles; mutant alleles have exclusively the (CAG)nC, whereas normal alleles have both (CAG)nG and (CAG)nC in a similar frequency[7,8] (Fig 1). Here, we engineered siRNAs to cleave selectively mutant MJD RNA targeting the sequence including this C/G polymorphism.

Materials and Methods

Plasmid Constructs and Small Interfering RNA Design

The expression plasmids of ataxin-3 were kindly given by Dr Akira Kakizuka.[4] The MJD1 cDNA in the plasmid was a truncated fragment including either 22 (normal, pCMX HA-Q22C) or 79 (expanded, pCMX HA-Q79C) repeats of CAG, and was hemagglutinin (HA)-fused on the N terminus. Cytosine after CAG repeat in pCMX HA-Q22C was changed to guanine (pCMX HA-Q22G) using the QuikChange site-directed mutagenesis system (Stratagene, La Jolla, CA). Furthermore, these MJD cDNAs also were subcloned into pIRES-hrGFP-1a (pGFP-Q22G, pGFP-Q22C and pGFP-Q79C; Stratagene).

Four different siRNAs were designed to target the mutant MJD RNA at the junction of CAG repeat and 3′ terminal region (see Fig 1B). A single nucleotide alternation at C/G polymorphism was placed in siRNA at 5th, 8th, 11th, or 14th position from the 5′ end of the sense strand.

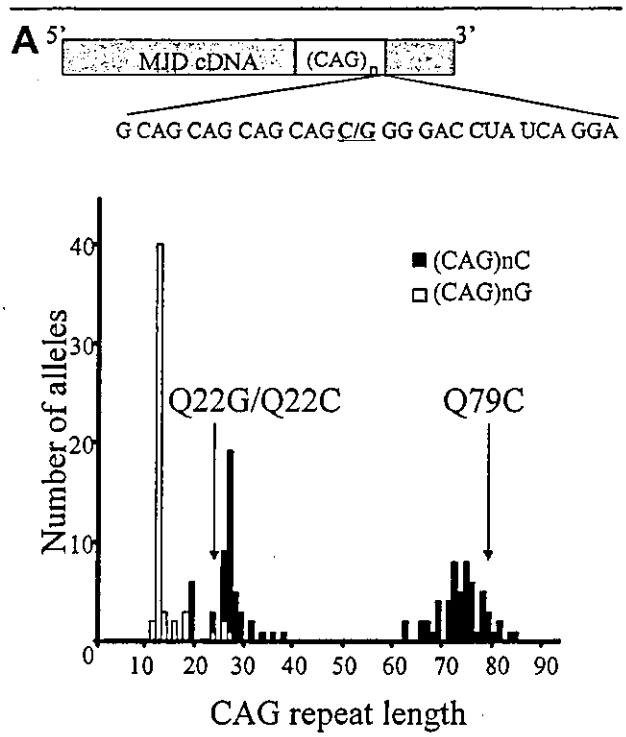

B

Name	Sequence
siRNA MJD1	5'- g cag cgg gac cua uca gga TT-3' 3'-TT c gac gcc cug gau agu ccu -5'
siRNA MJD2	5'- g cag cag cgg gac cua uca TT-3' 3'-TT c gac gac gcc cug gau agu -5'
siRNA MJD3	5'- g cag cag cag cgg gac cua TT-3' 3'-TT c gac gac gac gcc cug gau -5'
siRNA MJD4	5'- g cag cag cag cag cgg gac TT-3' 3'-TT c gac gac gac gac gcc cug -5'
Control (siRNA MJD3-shuffle)	5'- g gag agc aac gcg acc cguTT-3' 3'-TT c cuc ucg uug cgc ugg gca -5'

Fig 1. Design of small interfering RNA (siRNA) sequences targeting the C/G polymorphism in the Machado–Joseph disease (MJD)–1 gene (A) Schema of human MJD1 gene showing C/G polymorphism just downstream from CAG repeat (top panel). The distribution of C/G polymorphism and the CAG repeat length in 56 Japanese MJD patients (bottom panel). All expanded alleles have (CAG)nC, whereas the normal alleles have (CAG)nC and (CAG)nG in similar frequencies (0.46 and 0.54). Arrows indicate the CAG repeat numbers of ataxin-3 expression vector constructs used in this study as wild type and mutant. (B) Sequences of siRNAs used to target (CAG)nC in MJD1 mRNA. Bold characters indicate the site of C/G polymorphism. Uppercase letters indicate deoxyribonucleotides.

Transfections and Western Blotting

To see the effect of siRNAs for MJD RNA on the expression of ataxin-3, we cotransfected both siRNA and ataxin-3-expression plasmids to human embryonic kidney cell line

293T cells (293T) cells. siRNAs were annealed and transfected according to our previously reported method.[9] Four-microgram expression vectors and 10 or 25nM siRNA were cotransfected to 293T cells in six-well culture plates by Lipofectamine Plus reagent (Life Technologies, Rockville, MD).

Twenty-four hours after transfection, cells were harvested by TNG buffer (50mM Tris-HCl, 150mM NaCl, 1% Triton X-100) with protease inhibitor cocktail (Roche, Mannheim, Germany), separated on 15% sodium dodecyl sulfate polyacrylamide gels, and transfered onto polyvinylidene difluoride membrane (Bio-Rad, Richmond, CA). Rat monoclonal anti–HA antibody (Roche) was reacted and detected using an enhanced chemiluminescence detection kit (Amerham Pharmacia Biotech, Arlington Heights, IL).

Assessment of Cell Death

To assess the effect of siRNA on the cell death caused by expression of mutant ataxin-3, we cotransfected Neuro2a cells in 24-well culture plates with pCMX-Q79C (1μg/well) and siRNA (100nM/well). At 48 hours after transfection, the cell death of Neuro2a cells was determined by assaying with both trypan blue exclusion method and measurement of cytoplasmic lactate dehydrogenase (LDH) activity with the Cytotox 96 nonradioactive cytotoxicity assay (Promega, Madison, WI).

Statistical analysis were performed using the Student's *t* test and single-factor analysis of variance followed by Fisher's protected least-significant difference post hoc test.

Results

The mutant ataxin-3, Q79C, was most effectively suppressed by 25nM siRNA MJD3 and was decreased by 96.0% on signal intensity of Western blotting compared with that in control (Fig 2A). In contrast, the expression of the wild-type ataxin-3 Q22G was moderately suppressed by siRNA MJD4, but not clearly influenced by siRNA MJD1, -2, or -3. Therefore, siRNA MJD3 best recognized one nucleotide alternation between C and G and suppressed specifically expression of Q79C, with almost no effect on that of Q22G. Effect of siRNA MJD3 on Q79C expression was dose dependent, but suppression of Q22G was similar at 10 and 25nM concentrations of siRNA (see Fig 2B).

Unexpectedly, siRNA MJD3 did not significantly decrease (22.5%) the expression of another wild-type allele, Q22C, although the target sequence in (CAG)79C and (CAG)22C were the same (see Fig 2B). These suppression effects were confirmed by the reduction in fluorescence of GFP which was bicistronically expressed by internal ribosomal entry site (IRES) with ataxin-3 (pGFP-Q22C or pGFP-Q79C) using DsRed fluorescence as a control for transfection efficiency (see Fig 2C).

Next, by applying siRNA MJD3, we attempted to decrease the cell toxicity induced by mutant ataxin-3. Forty-eight hours after transfection, expression of the mutant MJD (Q79C) was toxic to Neuro2a cells, but those of the wild-type ataxin-3 (Q22G and Q22C) did not influence cell survival. siRNA MJD3 could markedly suppress the toxicity of mutant ataxin-3, decreasing cell death by 62.8% in LDH assay and by 75.9% in trypan blue exclusion method (Fig 3).

Discussion

This is the report of the siRNA which can discriminate mutant and wild-type type RNAs of MJD1 gene: the siRNA MJD3 is highly effective for suppressing mutant ataxin-3, Q79C, with a negligible effect on one wild-type ataxin-3, Q22G, observed in half of Japanese MJD patients, and with much less effect on the other wild-type allele, Q22C, in another half patients. The siRNA has been reported to suppress expression of the mutant androgen receptor RNA including expanded CAG repeat and rescue polyglutamine-mediated cytotoxicity, but it cleaved wild-type RNA with normal CAG repeat in a similar way.[10] During preparation of this article, Miller and his colleagues[11] reported the effective siRNA targeting the C/G polymorphism in MJD1 gene, which suppressed the Q166C expression with only modest effect on Q28G expression, but they did not examine another wild-type allele Q28C.

Diversing effects of mismatch between siRNA and target sequences have been reported. The central single mutation, mismatch in siRNA at 10th and 11th position, produces marked decrease of cleavage siRNA activity.[13] The mismatch in the 5′end has negligible effect on siRNA cleavage activity compared with more centrally located mutation. This bias might be linked to the proposed existence of a "ruler" region in the

Fig 2. Specific effect of the small interfering RNA (siRNA) on the expression of mutant MJD1. (A) Selection of best siRNA to discriminate C/G polymorphism. Western blot analysis of best siRNA for targeting mutant ataxin-3 among siRNA MJD1-4. 293T cells were cotransfected with ataxin-3 expression plasmids (pCMX HA-Q79C and pCMX HA-Q22G) and siRNAs. Tubulin loading controls also are shown. Right panel indicates quantitation of signal intensities. Each percentage suppression was determined by the band intensity with transfection of siRNA MJD3 shuffle as a control. siRNA MJD3 suppressed most Q79C expression, and siRNA MJD1-3 did not influence the Q22G expression. Values are the mean and SEM. (B) Comparison of the effect of siRNA MJD3 on Q79C, Q22G, and Q22C expression. Western blot analysis of the effect of siRNA MJD3 at 10 and 25nM on Q79C, Q22G, and Q22C expression. The results of siRNA(−) were made with siRNA MJD3 shuffle. Right panel indicates quantitation of signal intensities. Almost no suppression on Q22G expression (5.9%) and mild suppression on Q22C expression (22.5%) were noted by siRNA MJD3 at 25nM siRNA in contrast with robust suppression on Q79C expression (96.0%). Bottom panel shows the GFP images of 293T cells cotransfected with pGFP-Q79C/pGFP-Q22C/pGFP-Q22G and siRNA MJD3. pDsRed also was transfected as a control of transfection efficiency (×200).

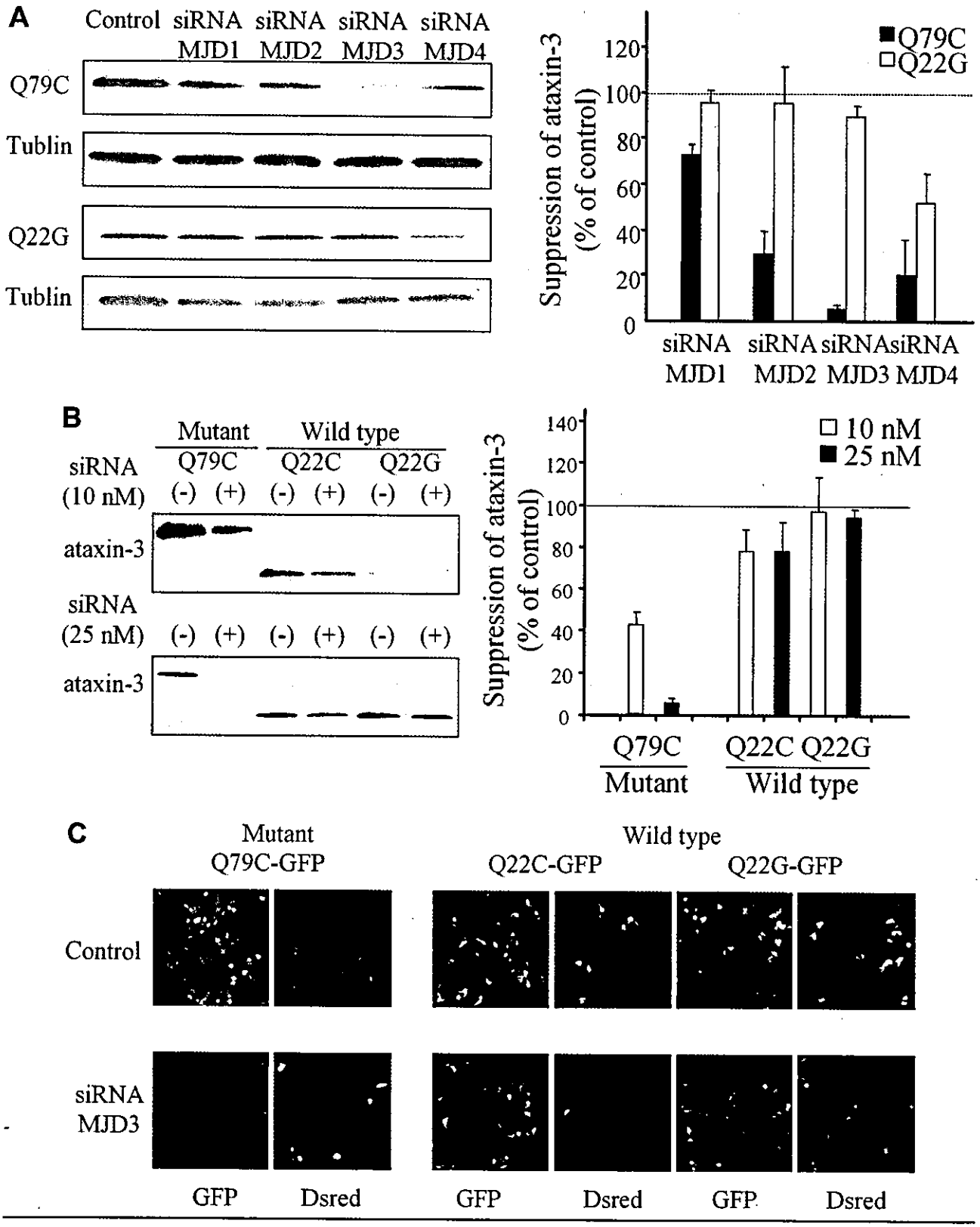
A
Control
siRNA MJD1
siRNA MJD2
siRNA MJD3
siRNA MJD4
Q79C
Tublin
Q22G
Tublin
Suppression of ataxin-3 (% of control)
Q79C
Q22G
siRNA MJD1
siRNA MJD2
siRNA MJD3
siRNA MJD4
B
Mutant
Wild type
siRNA (10 nM)
Q79C
Q22C
Q22G
ataxin-3
siRNA (25 nM)
ataxin-3
10 nM
25 nM
Suppression of ataxin-3 (% of control)
Q79C
Mutant
Q22C Q22G
Wild type
C
Mutant
Q79C-GFP
Wild type
Q22C-GFP
Q22G-GFP
Control
siRNA MJD3
GFP
Dsred
GFP
Dsred
GFP
Dsred

Figure 2

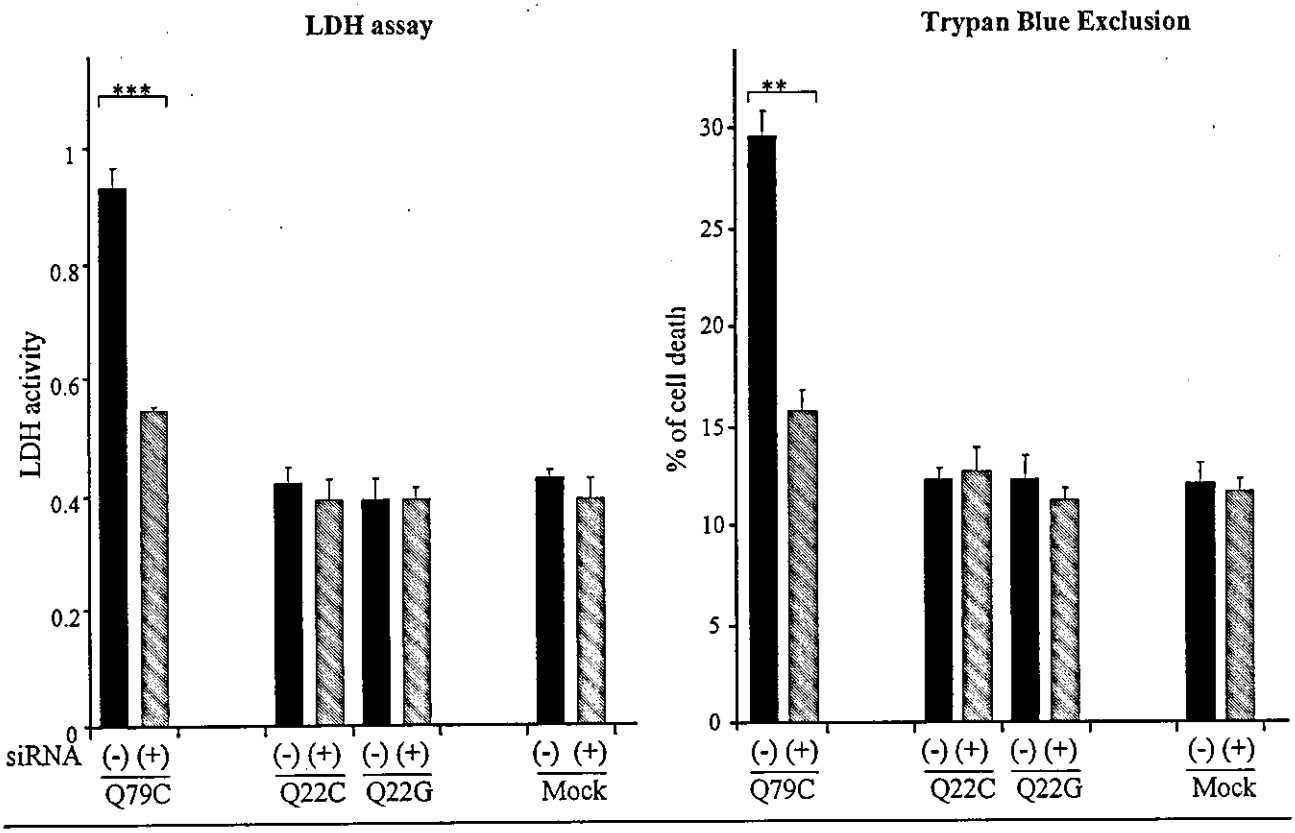

*Fig 3. Effect of small interfering RNA (siRNA) MJD3 on the mutant ataxin-3–induced toxicity in mammalian cells. siRNA MJD3 rescues the cell death induced by overexpression of Q79C, Q22C, and Q22G on lactate dehydrogenase (LDH) assay and trypan blue exclusion method (***$p < 0.0001$, **$p < 0.01$). Overexpression of Q22G or Q22C did not show toxicity. pcDNA3.1 plasmid (Invitrogen, La Jolla, CA) was used as mock. Values are the mean and SEM. The result of siRNA(−) was made with siRNA MJD3 shuffle.*

siRNA that is used by the RNA-induced silencing complex (RISC) complex to "measure" the target RNA for cleavage .[13] In four siRNAs examined in our study, siRNAs (siRNA MJD2 and -3) with central mismatch have better discrimination than that with outside mismatch (siRNA MJD1 and -4), and this result is consistent with the previously reported results.

Surprisingly, there was much difference between the effect of siRNA on Q22C and Q79C, although their target sequences of siRNAs were the same. This is the first report to our knowledge of sequence-independent discrimination of mutant and wild-type alleles by siRNA. One possible reason for this difference is that not all RNA sequences are equally accessible to siRNAs: some sequences might be buried within the secondary structure of target RNAs especially when they are highly folded.[15] We also experienced that the best target site of siRNA for the highly folded RNA was almost same as that for ribozyme, which cleavage efficiency is much influenced by the secondary structure of target RNA.[9] The target site of C/G polymorphism is just downstream from the CAG repeat, which represents a tight stem form in their secondary structure on a computer prediction. Although we have no data indicating that siRNA MJD3 is more accessible to (CAG)79C than (CAG)22C, a change of secondary structure of the MJD RNA due to a large difference of the CAG repeat length might affect the efficiency of siRNA MJD3. Another possible explanation is that there is a RNA-binding protein preferentially binding (CAG)22C over (CAG)79C, which interferes the access of siRNA MJD3 to (CAG)22C RNA. The RNA-binding protein to MJD RNA has not been found, but CUG repeat in myotonic dystrophy protein kinase (DMPK) RNA binds the proteins including CUG-binding protein in repeat length-dependent manner.[15] Moreover, existence of a RNA-binding protein attaching CAG repeat was suggested in Huntington's disease.[16] Further studies are needed to make clear the mechanism for the difference of the siRNA effect on (CAG)79C and (CAG)22C.

We are in the process of making adeno-associated virus and transgenic mice expressing siRNA MJD3 to investigate the efficacy of siRNAs in vivo. Although a less invasive delivery method for introducing siRNAs into a larger area of cerebellum would be needed for clinical feasibility, the efficiency of our siRNA to specifically reduce the expression and toxicity of mutant

ataxin-3 in cells suggests that this mRNA-targeting approach by siRNA might provide effective therapy for MJD.

This work was supported by grants from the Ministry of Education, Science and Culture of Japan (14570582; T.Y.) and from the Ministry of Health, Labor and Welfare of Japan (H14-KOKORO-018; T.Y.), and 21st Century Center of Excellence (COE) Program Fellowship (L.Y.).

We thank Dr A. Kakizuka for providing expression vectors of MJD gene.

References

1. Kawaguchi Y, Okamoto T, Taniwaki M, et al. CAG expansions in a novel gene for Machado-Joseph disease at chromosome 14q32.1. Nat Genet 1994;8:221–228.
2. Ross CA. When more is less: pathogenesis of glutamine repeat neurodegenerative diseases. Neuron 1995;15:493–496.
3. Ikeda H, Yamaguchi M, Satoshi S, et al. Expanded polyglutamine in the Machado-Joseph disease protein induced cell death in vitro and in vivo. Nat Genet 1996;13:196–202.
4. Kobayashi T, Tanaka K, Inoue K, Kakizuka A. Functional ATPase activity of p97/valosin-containing protein (VCP) is required for the quality control of endoplasmic reticulum in neuronally differentiated mammalian PC12 cells. J Biol Chem 2002;277:47358–47365.
5. Wang G, Sawai N, Kotliarova S, et al. Ataxin-3, the MJD1 gene product, interacts with the two human homologs of yeast DNA repair protein RAD23, HHR23A and HHR23B. Hum Mol Genet 2000;9:1795–1803.
6. Elbashir S, Harborth J, Lendeckel W, et al. Duplexes of 21 nucleotide RNAs mediate RNA interference in cultured mammalian cells. Nature 2001;411:494–498.
7. Matsumura R, Takayanagi T, Murata K, et al. Relationship of (CAG)nC configuration to repeat instability of the Machado-Joseph disease gene. Hum Genet 1996;98:643–645.
8. Gaspar C, Lopes-Cendes I, Hayes S, et al. Ancestral origins of the Machado-Joseph disease mutation: a worldwide haplotype study. Am J Hum Genet 2001;68:523–528.
9. Yokota T, Sakamoto N, Enomoto Y, et al. Inhibition of intracellular hepatitis C virus replication by synthetic and vector-derived small interfering RNAs. EMBO Rep 2003;4:602–608.
10. Caplen NJ, Taylor JP, Statham VS, et al. Rescue of polyglutamine-mediated cytotoxicity by double-stranded RNA-mediated RNA interference. Hum Mol Genet 2002;11:175–184.
11. Miller VM, Xia H, Marrs GL, et al. Allele-specific silencing of dominant disease genes. Proc Natl Acad Sci USA 2003;100:7195–7200.
12. Elbashir SM, Martinez J, Patkaniowska A, et al. Functional anatomy of siRNAs for mediating efficient RNAi in *Drosophila melanogaster* embryo lysate. EMBO J 2001;20:6877–6888.
13. Holen T, Amarzguioui M, Wiiger MT, et al. Positional effects of short interfering RNAs targeting the human coagulation trigger tissue factor. Nucleic Acids Res 2002;30:1757–1766.
14. Yoshinari K, Miyagishi M, Taira K, et al. Effect on RNAi of the tight structure, sequence and position of the targeted region. Nucleic Acids Res 2004;32:691–699.
15. Philips AV, Timchenko L, Cooper TA. Disruption of splicing regulated by a CUG-binding protein in myotonic dystrophy. Science 1998;280:737–741.
16. McLaughlin BA, Spencer C, Eberwine J. CAG trinucleotide RNA repeats interact with RNA-binding proteins. Am J Hum Genet 1996;59:561–569.

